Title
Evaluating the Utility and Usability of Palatal Plane in 2D and 3D

Permalink
https://escholarship.org/uc/item/5rx1t6p2

Author
Yoon, Stephan Suksong

Publication Date
2016

Peer reviewed|Thesis/dissertation

Evaluating the Utility and Usability of Palatal Plane in 2D and 3D

by

Stephan S. Yoon, DMD.

THESIS

Submitted in partial satisfaction of the requirements for the degree of

MASTER OF SCIENCE

in

Oral and Craniofacial Sciences

in the

GRADUATE DIVISION

of the

UNIVERSITY OF CALIFORNIA, SAN FRANCISCO

DEDICATION

I would like to dedicate this Master's Thesis to my parents, Yoo-Joong John Yoon and Young-Eun Eunice Yoon. I would not be the person I am today without their love, support, and sacrifice.

ACKNOWLEDGEMENTS

I would like to thank Dr. Arthur Miller for his patience with guiding me through every step of executing this study and writing it out. This project truly would not have been possible without his support and accountability.

I would like to thank Dr. Gerald Nelson for genuinely caring for my learning and experience with the research project. His expertise on CBCT was invaluable for this project.

I would like to thank Dr. Steven Frank his enthusiasm and support of this project. Dr. Frank was important in brining Ricketts ideas to the study.

I would like to thank Dr. Kjeld Aamodt for generously offering his help with the project and thesis. It was very helpful to have a mentor who has gone through the same process recently.

I would like to thank Dr. Seong-Hun Kim for inspiring me with his passion to advance orthodontics and pitching me the research project idea. Despite being on the other side of the globe, he continued to teach, support, and challenged me.

ABSTRACT

Evaluating the Utility and Usability of Palatal Plane in 2D and 3D

Stephan S. Yoon, DMD

Background and Objective: The purpose of the study is to evaluate the utility of the palatal plane in both 2D and 3D. The first aim is to study and compare the correlation between the sella nasion-to-mandibular plane angle (SN-MP), to the palatal plane-to-mandibular plane angle (PP-MP), and open bite tendency. The second aim is to develop a method of identifying the palatal plane, mandibular plane, and associated landmarks in 3D on CBCT. The third aim is to test and compare the reliability of landmarks identification involved in palatal plane, mandibular plane, and associated measurements in 3D and 2D. The last aim is to evaluate the difference between the palatal and mandibular plane associated measurements identified from the 3D CBCT analysis and 2D lateral cephalographs.

Materials and Methods: Aim 1: 50 subjects in permanent dentition were randomly chosen at UCSF. Their lateral cephalographs were collected to measure and compare the correlation between SN-MP, PP-MP, and overbite. Aim 2: A protocol was developed to use a hybrid between volumetric rendering and multi-planar reconstruction to trace palatal plane, mandibular plane, and associated measurements in 3D using Anatomage Invivo5. Aim 3: Precision of the landmarks were compared between 3D tracing on CBCT and 2D lateral cephalographs, both overall as well as per individual axis. Aim 4: associated measurements, PP-MP, U1-PP, and L1-MP, were measured and compared between 3D and 2D tracings.

Results: There was a strong correlation between SN-MP and PP-MP (R= 0.859) and no significant difference between SN-MP to open bite and PP-MP to open bite. Generally, landmark

identification was significantly more precise in 3D tracing than 2D tracing (0.549mm vs 1.440mm). In 3D, tracing was more precise in Y-axis than X-axis (0.168mm vs 0.367mm), whereas in 2D, it was more precise in X-axis than in Y-axis (0.640mm vs 0.823mm). Incisor crown tips ranked high on precision ranking in both 3D and 2D. and PNS ranked low in both 3D and 2D, while root apices ranked higher on 3D than in 2D. U1-PP measurements in 3D were significantly lower than that of 2D (-3.73 degrees), L1-MP measurements in 3D were significantly higher than that of 2D (+2.35 degrees), but PP-MP measurements did not significantly differ between 3D and 2D.

Conclusions: PP-MP, similar to SN-MP, is valuable in evaluating vertical jaw relationship and open bite tendencies. Overall, landmark identification in 3D is significantly more reliable and precise than in 2D. However, the patterns of precision differ between different landmarks and different axes. Measurements such as U1-PP and L1-MP significantly differ when measured in 3D compared to 2D.

Key words: CBCT, lateral cephalographs, landmark tracing, reliability, precision, consistency, palatal plane, and mandibular plane.

TABLE OF CONTENTS

LIST OF TABLES

LIST OF FIGURES

INTRODUCTION

The invention of computed tomography (CT) was a break through in radiographic imaging for it allowed clinicians to evaluate the depths of the human anatomy, slice by slice, through computer reformation of radiographic images. (1) While introducing computed tomography to head and neck anatomy opened opportunities to be more creative, comprehensive, and precise in evaluating craniofacial structures, these were not realistically obtainable due to high cost and biological burden on the patient resulting from high radiation exposure. This problem was greatly addressed by the rather recent introduction of cone-beam computed tomography (CBCT), which due to its single rotation of the x-ray tube, both decreases the radiation exposure and reduces blurring of the image from patient movement during image capturing. (2, 3, 4)

Since being first introduced in 1990's, both the technology of capturing CBCT and the ability and knowledge to manipulate and interpret CBCT have advanced exponentially. (2) Currently, scan time can be as low as 9 seconds and radiation exposure as low as 40-50mSv, which is comparable to full mouth series of dental x-rays. (5) As CBCT technology advances, companies are developing ultra low dose scans with radiation of under 15mSv.

Generating 2D images from CBCT

From CBCT, an operator can obtain the familiar 2D images more accurately and efficiently. Bilateral structures are often overlapped in 2D cephalometric images, blurring the final image when there is asymmetry in the patient or patient's head was tilted at the time of capturing the image. Commonly found example of this is gonial angles and mandibular planes determined by selected gonial angles. When right and left gonial angles are not clearly

1

superimposed, clinicians will often select an arbitrary middle point to address this, introducing more variability to the associate measurements. (6, 7) With CBCT, if a patient's head position is unintentionally tilted, it can be corrected by simply reorienting the image, which allows more accurate superimposition of bilateral structures. (8) In the presence of true asymmetry, the right and left sides of the craniofacial structures can be evaluated individually and compared to each other. (9) Other various types of routinely acquired 2D radiographs can be obtained from CBCT such as panographs or PA cephalographs. Similarly to lateral cephalographs, panographs and PA cephalographs can be generated from correct head orientation of CBCT.

Advantage of acquiring familiar 2D images is that one can utilize the findings and evidences from years of research to interpret the images. (10)

Utilization of CBCT

Benefits of CBCT extend well beyond the advantage of generating more accurate 2D images from it. More magnified and higher resolution incremental slices can be generated in an area of interest such as impacted canines or concern for pathology or abnormality. Additionally, ability to maneuver around volumetric rendering of CBCT allows the operator to evaluate root position in multi-dimensions simultaneously. For example, severely proclined incisors that may be misinterpreted on conventional 2D panographs for having shortened roots, will be correctly evaluated when examined in 3D volumetric rendering. (8, 9)

Furthermore, CBCT can be used for 3D visual treatment objectives development, superimposition, and 3D analyses. Good CBCT analyses should continue to utilize measurement norms established from previous 2D lateral ceph studies, but also incorporate truly 3D measurements. (8) Such analyses and measurements have been in active development in past

years and are being tested for their usefulness

In order to achieve quantitative assessment using CBCT, reliable landmarks and analyses using associated measurements need to be established. Good analyses should continue to utilize measurement norms established from previous 2D lateral ceph studies, but also include new measurements that take advantage of the third dimension in CBCT. (8, 9) However, while there have been several studies that evaluated the reliability of landmark identification and measurements in lateral headfilms, similar studies on 3D are few, especially ones that directly compare reliability of the two imaging options on same subjects. (6, 7, 11)

Reliability of Landmark Identification

A landmark, anatomical or artificial, cannot be a good candidate if different individuals cannot reliably trace it repeatedly. For this reason, the reliability of landmark identification has been studied since the beginning of 2D lateral cephalograph tracing. (12) Baumrind *et al.,'s* study from University of California, San Francisco, was one of the first studies that evaluated the reliability of commonly used landmarks in 2D lateral cephalograph tracing. (6, 7) Several studies list errors in landmark identification as one of the main causes for error in cephalograph analyses along with others such as projection error, mechanical error in drawing lines between points on tracing, and error in measuring the angles or distances (10). While computer softwares eliminate the latter reasons for error, the errors in tracing landmarks still exist despite best efforts to automate the tracing by computers. Baumrind's study as well as several that followed showed that landmark tracing error varies between different landmarks and in different axes (x-axis vs y-axis). (13) These findings are important in the transitioning from 2D cephalograph to 3D CBCT in order to identify landmarks that are more difficult to reliably identify in 3D. Such landmarks

would result in errors measurements, both angular and linear, and, therefore, should be considered to be excluded in the list of landmarks to be used for 3D analyses. Equally as important as the landmarks to be traced is the method by which 3D tracing is executed. Two major methods are using volumetric rendering and multiplanar reconstruction (MPR). Tracing a point on volumetric rendering is faster for gross tracing but may not be precise, whereas, using MPR allows more precise tracing but is more time consuming.

Palatal Plane

The palatal plane is a reference plane often used in different ceph analyses measurements such as upper incisor inclination-to-palatal plane (U1-PP). As a reference plane, palatal plane has an advantage over others such as the sella-nasion line and Frankfort horizontal lines in that it is closer to the maxillomandibular complex. The closer proximity to maxillomandibular complex makes it a useful reference plane in CBCT with limited field of view such as a reset or progress radiograph. In non-growing patients, the palatal plane can even be used to for superimpositions.

When evaluating skeletal vertical jaw relationship and open bite tendency, SN-MP is most commonly used. However, the literature to compare the usefulness of SN-MP and PP-MP in evaluating vertical jaw relationship is lacking. It is possible that PP-MP is similarly as effective as SN-MP in assessing open bite tendency, if not more, and such finding will raise the value of palatal plane.

The palatal plane, despite its name, has traditionally been used as a line on 2D cephalometric analysis. In 3D CBCT, however, the palatal plane should be identified as a 3D structure, which increases the utility of it but also creates a new challenge of tracing a 3D palatal

plane. The advantage is that all the previously used measurements using the palatal plane can be measured more accurately using the anatomically accurate CBCT material. In asymmetric patients, the operator no longer needs to guess the palatal plane but can accurately depict it. Precise identification of both palatal and mandibular planes in 3D will provide more anatomically accurate measurements. Additionally, the palatal plane can also be used from the anteroposterior (AP) assess transverse jaw relationship and determine maxillary cant in relation to cranial base as well as the occlusal plane and mandibular plane. The challenge will be with assigning additional landmarks in addition to ANS and PNS to create a plane in 3D. As discussed, these landmarks need to be reliably traceable.

Purpose of the Study

The purpose of the study is to evaluate the utility of the palatal plane in both 2D lateral cephalographs and 3D cone beam computed tomography (CBCT).

Specific Aims

1. To study and compare the correlation between sella nasion-to-mandibular plane angle (SN-MP) and the palatal plane-to-mandibular plane angle (PP-MP), and open bite tendency.

2. To develop a method of identifying the palatal plane, mandibular plane, and associated landmarks in 3D on CBCT.

3. To test the reliability of 3D landmarks identification involved in palatal plane, mandibular plane, and associated measurements.

4. To evaluate the difference between the palatal and mandibular plane associated measurements identified from the 3D CBCT analysis and 2D lateral cephalographs.

HYPOTHESES

1. There is no significant difference between correlation between SN-MP and over bite and correlation between PP-MP and over bite.

2. There is no significant difference between reliability of same landmarks identification 3D CBCT and 2D lateral cephalographs.

3. There is no significant difference between palatal and mandibular plane associated measurements between 3D CBCT and cephalograph tracing.

METHODS AND MATERIALS

Aim 1: To study and compare correlation between sella nasion-to-mandibular plane angle (SN-MP), palatal plane-to-mandibular plane angle (PP-MP), and open bite tendency.

Inclusion criteria

      50 subjects were chosen at random from patients who came to UCSF orthodontic clinic for beginning record between the dates of July 2013 to July 2015. All permanent teeth except second molars must have erupted into oral cavity.

Exclusion criteria

      Subjects were excluded if they have history of previous orthodontic treatment or a diagnosis of craniofacial anomaly.

      Lateral cephalographs were taken on Carestream 9300 (Atlanta, GA). Images were imported to and traced on Dolphin Imaging (Chatsworth, CA) (Figure 1). The landmarks traced and measurements collected were as follow:

      Landmarks: sella, nasion, anterior nasal spine (ANS), posterior nasal spine (PNS), menton, gonion, upper incisor tip, upper incisor root, lower incisor tip, and lower incisor root.

      Measurements: SN-MP angle, PP-MP angle, and over bite.

Three correlation studies were conducted between the measurements: SN-MP vs PP-MP, SN-MP vs overbite, and PP-MP vs overbite.
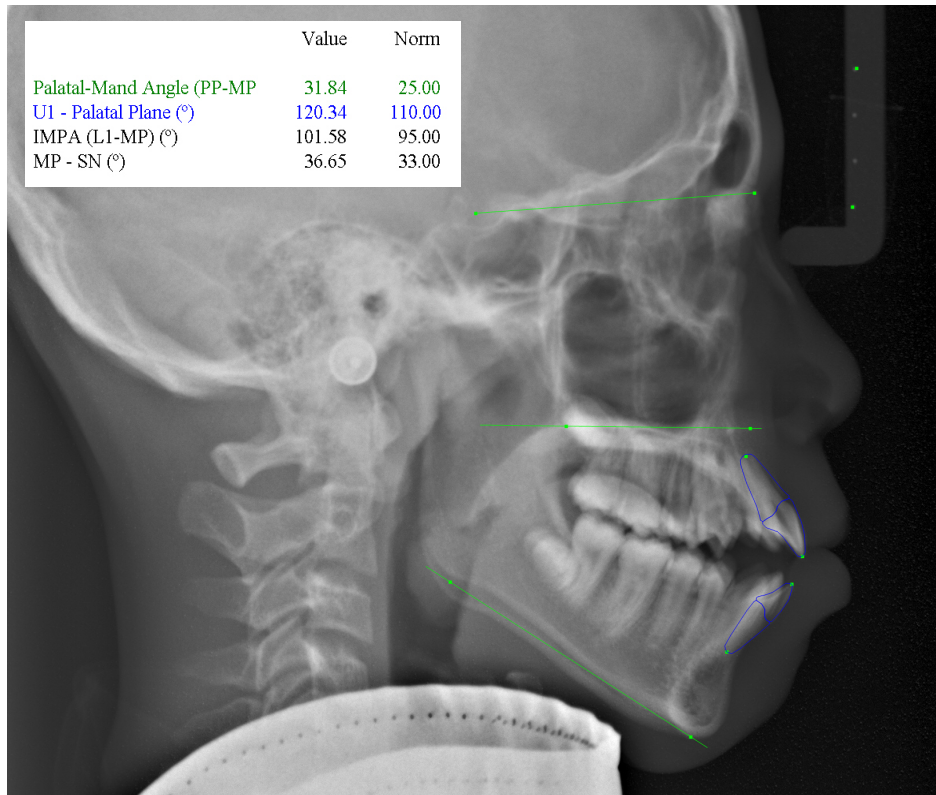
Figure 1: Lateral cephalograph traced with sella, nasion, ANS, PNS, upper incisor tip/apex, and lower incisor tip/apex.

Aim 2: To develop method of identifying the palatal plane, mandibular plane, and associated landmarks in 3D on CBCT.

CBCT

All of the images were captured by a single dental radiology technician at UCSF using Carestream 9300. Patients were standing upright during the capture of CBCT. Images were captured and exported as DICOM files.

Tracing

DICOM files were imported to and traced on Anatomage Invivo5 (San Jose, CA). An hybrid of 3D volumetric rendering and multi-planar reconstruction (MPR) was used as method of tracing. The 3D volumetric rendering mode makes it easier for the operator to visualize and

navigate around the image (Figure 2). Multi-planar reconstruction allows more precise tracing via displaying the traced landmark in all three planes: sagittal, coronal, and transverse. However, it had the disadvantage of taking longer (Figure 3). In combining of the two methods, the operator is able to perform quick initial gross tracing via volumetric rendering, then fine-tune the point by adjusting in MPR mode as needed (Figure 4). Most landmarks were traced using this approach except PNS. Since it is an internal structure, PNS is difficult to visualize in volumetric rendering. Therefore, initial gross tracing of PNS was placed on sagittal slice generated at midline (Figure 5). The angle of the view in volumetric reconstruction mode was customized for each landmark to make initial gross tracing simpler (Figure 4).

Figure 2: 3D volumetric rendering is easier to visualize and navigate through.
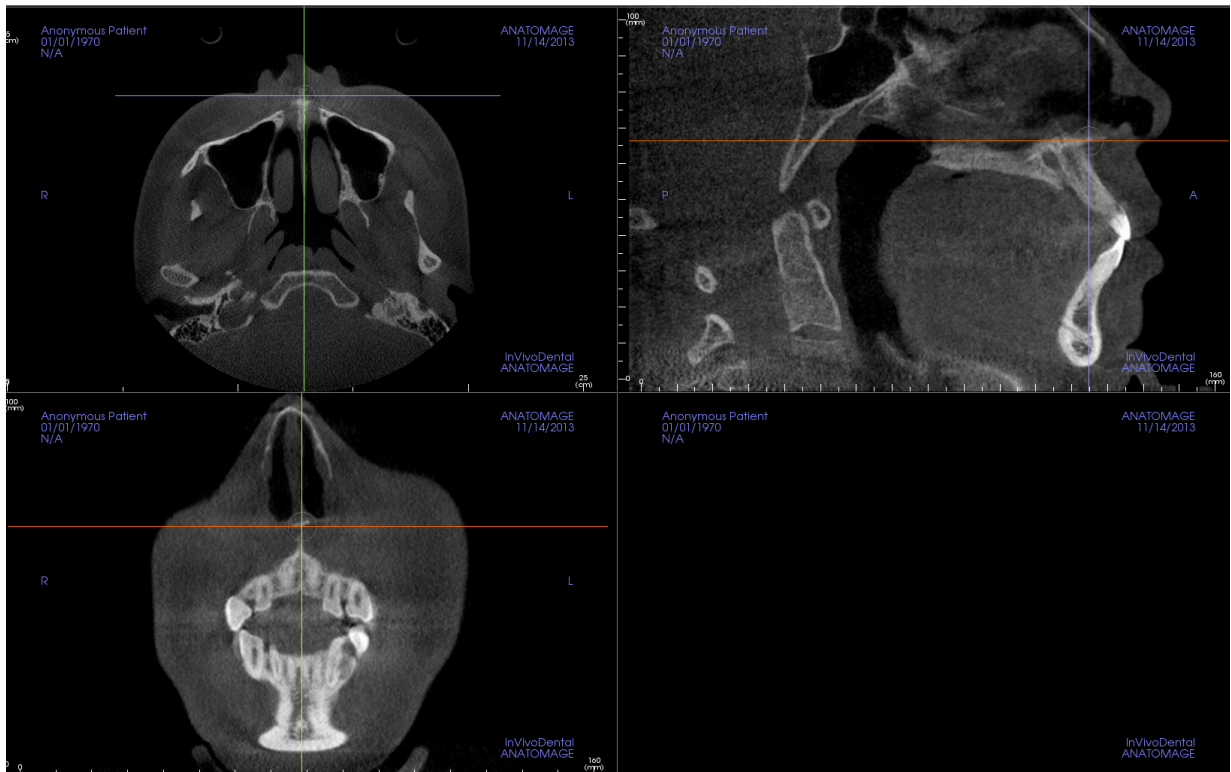
Figure 3: Multi-planar reconstruction (MPR) allows view in three different planes.
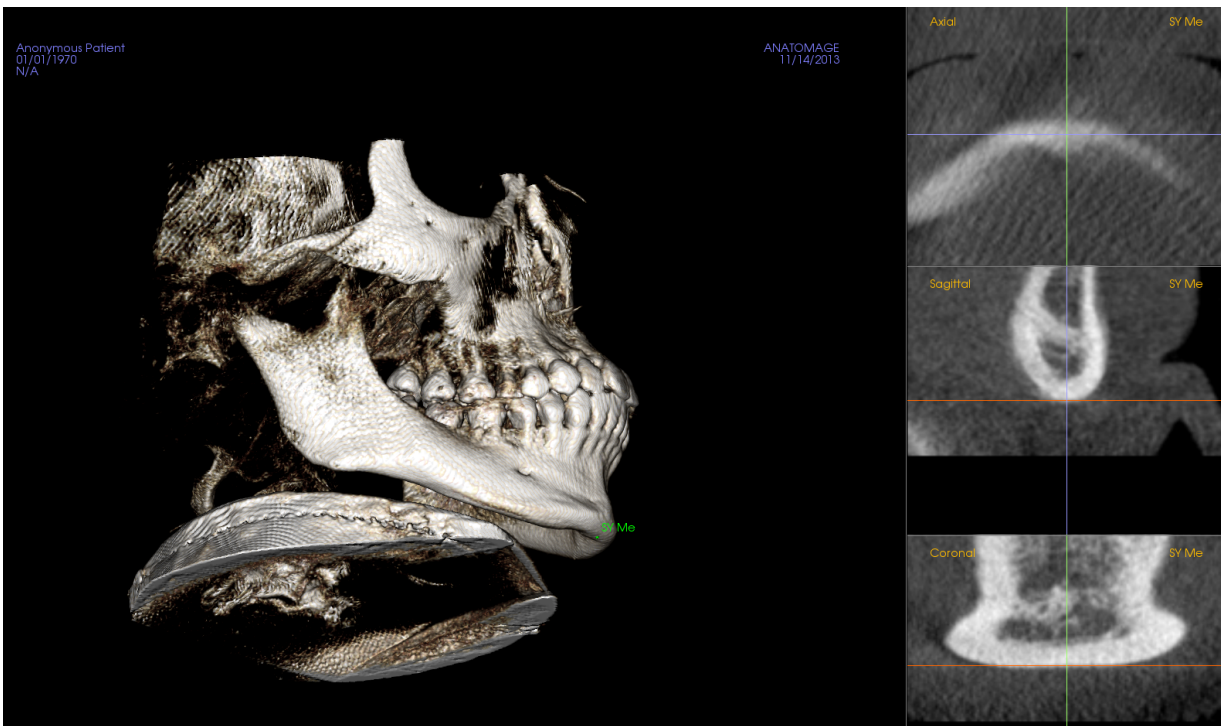
Figure 4: Hybrid of volumetric rendering and multi-planar reconstruction allows quick initial gross tracing followed by fine-tuning in MPR view.
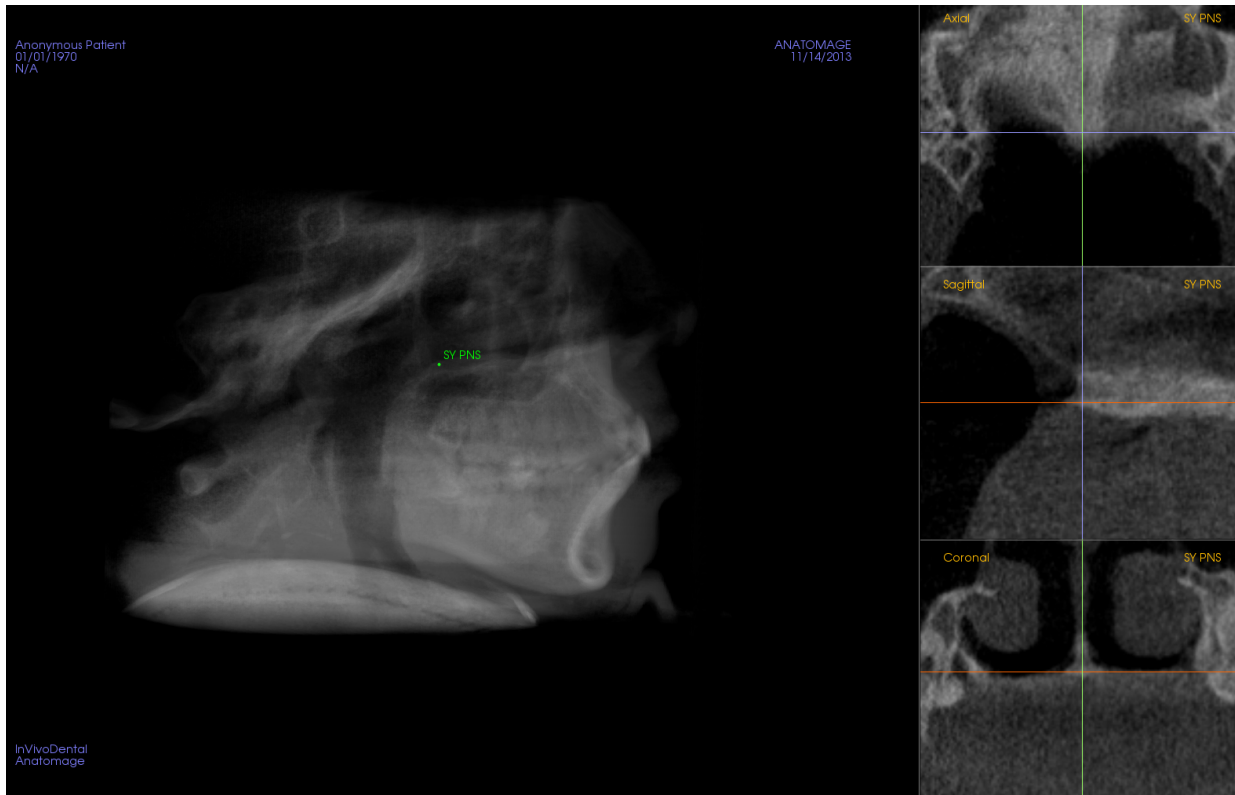
Figure 5: PNS, due to being an internal structure, is easier to perform initial tracing on sagittal radiograph than on volumetric rendering.

Landmarks

15 landmarks were included in the CBCT tracing, 8 bilateral landmarks and 7 non-bilateral landmarks.

Table 1: 15 landmarks for CBCT tracing

Landmark	Definition
J-point R/L	The most concave point on the most lateral border of the maxilla near maxillary second molars
ANS	The tip of the anterior nasal spine
PNS	The tip of the posterior nasal spine
Menton	The most inferior point of the symphysis

Gonion R/L	Most convex point where the posterior inferior curve of the ramus meets.
Antegonial notch R/L	Point at the lateral inferior margin of the antegonial protuberance.
UR1 crown tip	Incisal tip of the upper central incisors
UR1 root apex	Root apex of the upper central incisors
LR1 crown tip	Incisal tip of the lower central incisors
LR1 root apex	Root apex of the lower central incisors
Orbitale R/L	The deepest point of the infraorbital margin

What are referred to as palatal and mandibular planes in traditional 2D lateral cephs are actually lines rather than true planes, and, therefore, require only two landmarks each to define them. ANS and PNS define palatal plane and menton and gonion define mandibular plane. However, in order to construct a true plane in 3D, more than two points are required.

Mandibular plane

A plane can be defined by three points that are not in a straight line. Since the gonions are bilateral structures, menton, right gonion, and left gonion were selected to form a mandibular plane (Figure 6).
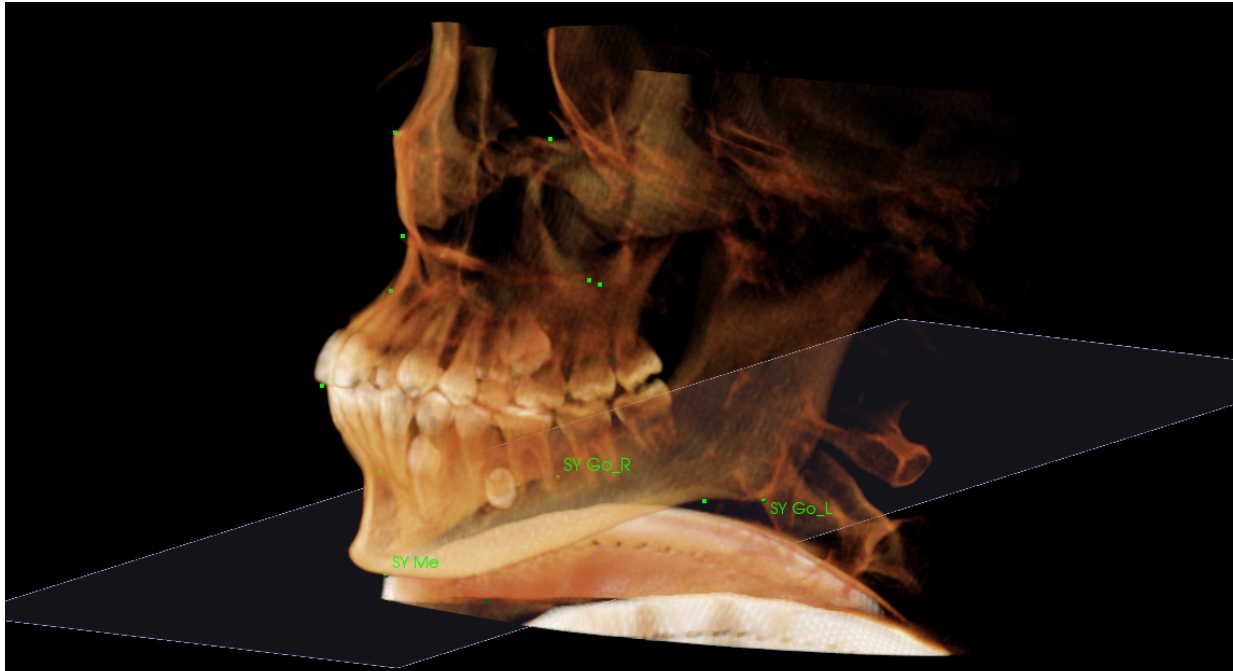
Figure 6: Mandibular plane in 3D determined by menton and right/left gonion.

Palatal plane

The palatal plane, similar to the mandibular plane, is not an actual anatomical plane. However, while the mandibular plane includes bilateral structures, the palatal plane does not as ANS and PNS are both midline structures. Therefore, bilateral landmarks are needed to be selected to determine palatal plane. The purpose of the bilateral structures is to determine the "roll" of the plane that includes ANS and PNS. An illustration of an airplane depicts this more clearly (Figure 7). After considering several different candidates, J-points were selected as the bilateral structures for a few reasons. First, J-points are closer to the palatal plane in comparison to other bilateral landmarks considered, such as the infraorbital foramen. Secondly, J-points are not significantly affected by the eruption status of the posterior teeth, such as the height of dentoalveolar bone. Lastly, J-points can be used to evaluate the transverse discrepancy between maxilla and mandible. J-points have been used in several AP cephalometric analyses, such as in

Ricketts analysis, along with antegonial notch-to-antegonial notch line to quantitatively measure

the transverse discrepancy between maxilla and mandible (Figure 8).
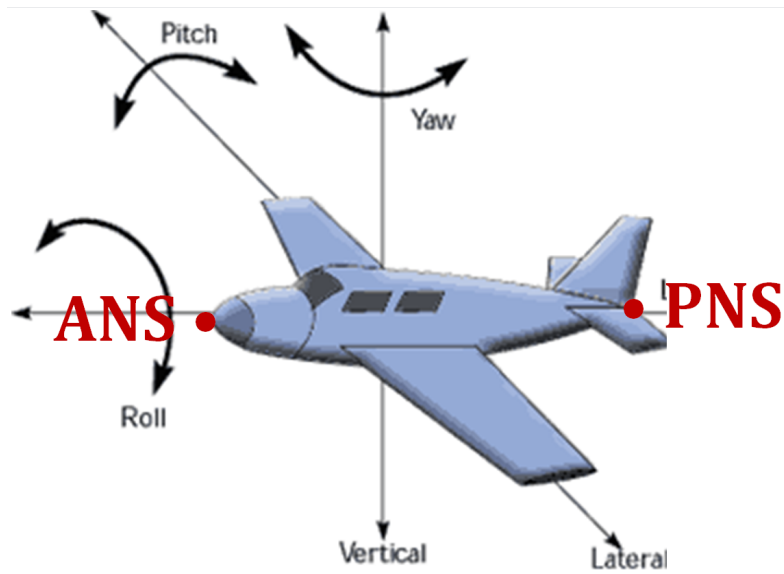
Figure 7: Depiction of palatal plane via airplane model. ANS and PNS are represented by the head and tail of the airplane. Bilateral structures are needed to determine the "roll" of the palatal plane.
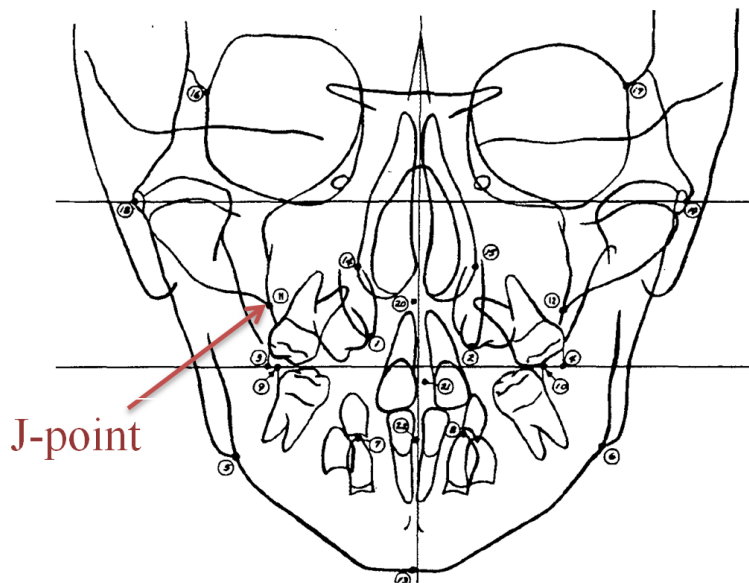
Figure 8: Ricketts PA cephalograph tracings included J-points.

Together, the palatal plane is defined as a plane that passes through ANS and PNS, and these landmarks are equidistant from right and left J-points (Figure 9). J-points were defined as the most concave point on the most lateral border of the maxilla near the maxillary second molars (Figure 10). Ricketts has similarly described these points as points on jugal process at the intersection of the outline of the tuberosity and zygomatic buttress (Ricketts, 1961).
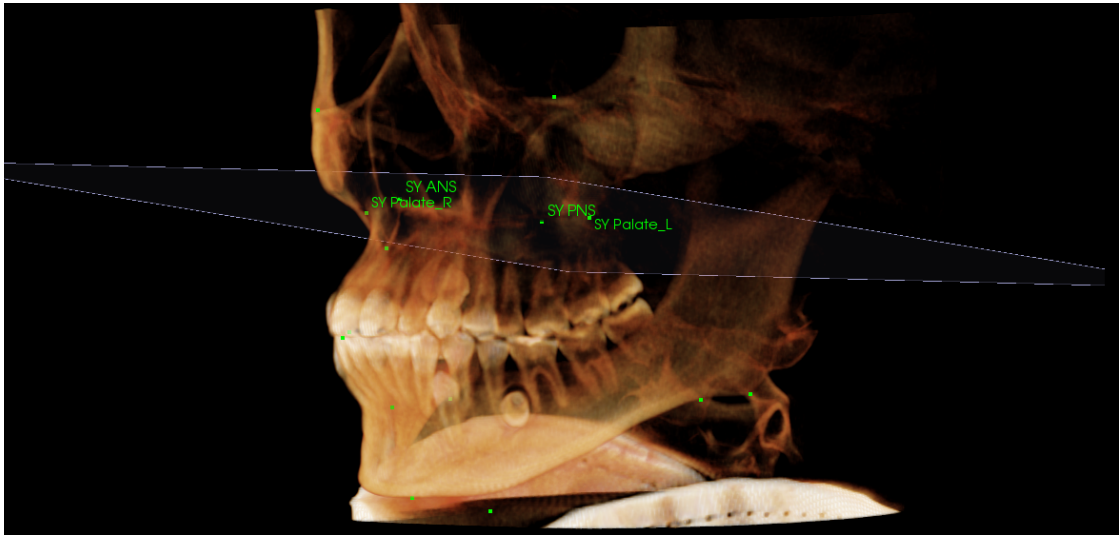
Figure 9: Palatal plane in 3D determined by ANS, PNS, and right/left J-points.
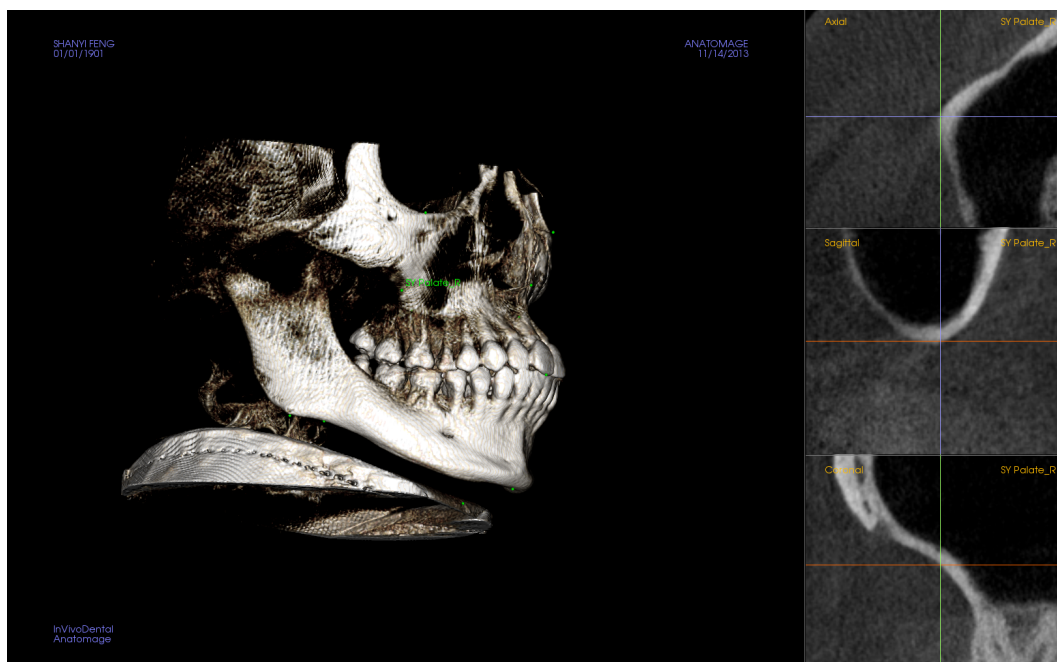
Figure 10: J-point

Once the two planes are determined in 3D, the true palatal plane to mandibular plane angle can be visualized and measured (Figure 11)
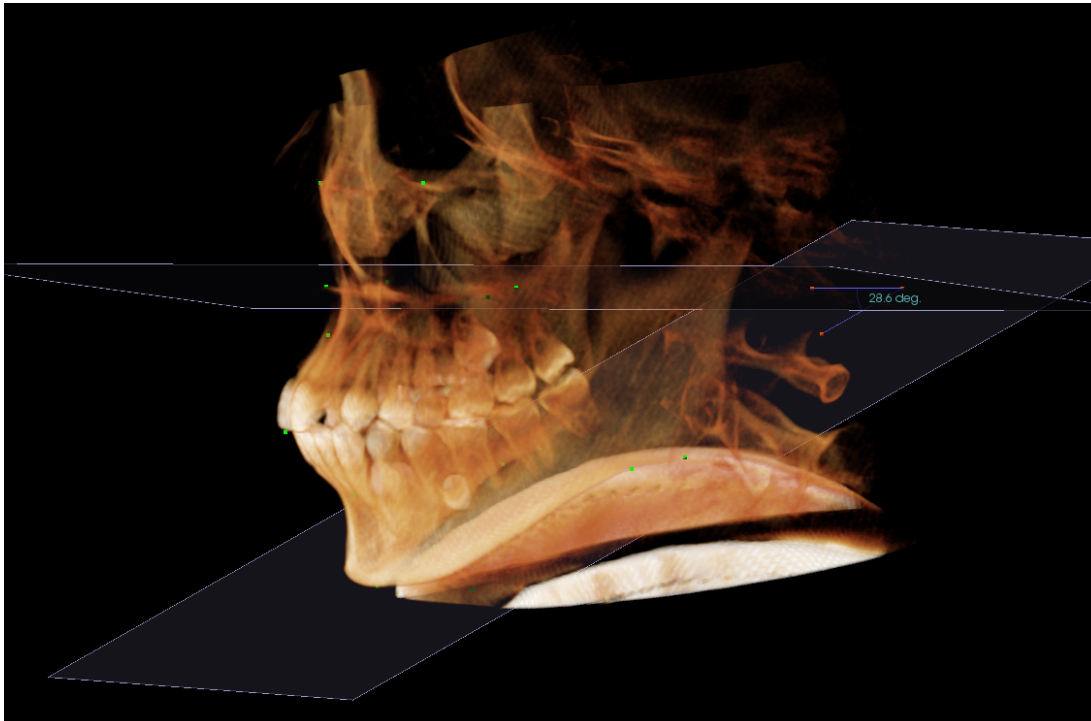
Figure 11: True palatal plane-to-mandibular plane angle, PP-MP.

Incisor inclination

In order to evaluate incisor inclination of upper and lower incisors relative to palatal and mandibular plane respectively (U1-PP, L1-MP), the long axis of upper right central incisors and lower right central incisors were determined by identifying the crown tip and root apex. Overlap of multiple incisors in lateral cephalographs often creates challenge to identify incisor angulation accurately. CBCT tracing eliminates this variability by isolating and selectively tracing an individual tooth (Figure 12). For the purpose of this study, upper right central incisors were used, but other incisors can be added or substituted as desired in subsequent models.
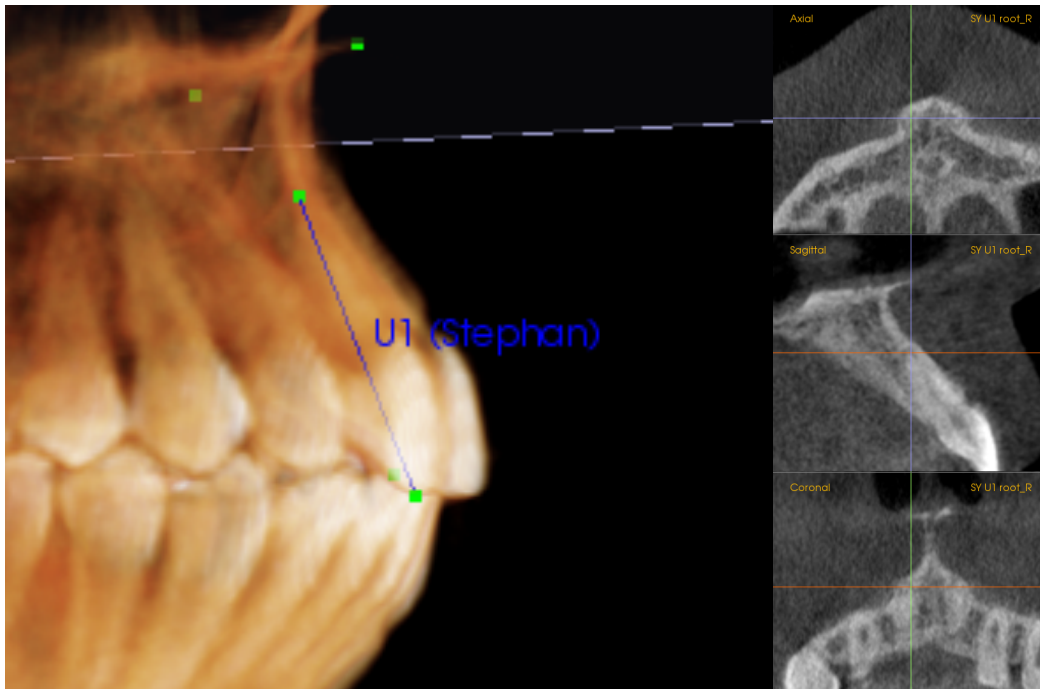
Figure 12: Long axis of UR1 determined by the tooth's crown tip and root tip, and its relationship to palatal plane (U1-PP).

Frontal evaluation for cant and symmetry

J-points are used to evaluate symmetry and cant of the maxilla/palatal plane and the mandible in relation to each other and to cranial base (Figure 13). The horizontal cant of the cranial base is determined by connecting right and left orbitales.   The horizontal cant of the mandibular plane is determined by connecting right and left gonion. The cants of cranial base, palatal plane, or mandibular plane are visualized and measured. Additionally, Ricketts has shown that on average, width of antegonial notch-to-antegonial notch is about 10mm greater than J-point to J-point. Deviation from 10mm difference indicates maxillary width excess or deficiency. Difference between antegonial notch-to-antegonial notch and J-point to J-point are automatically computed in the analysis.
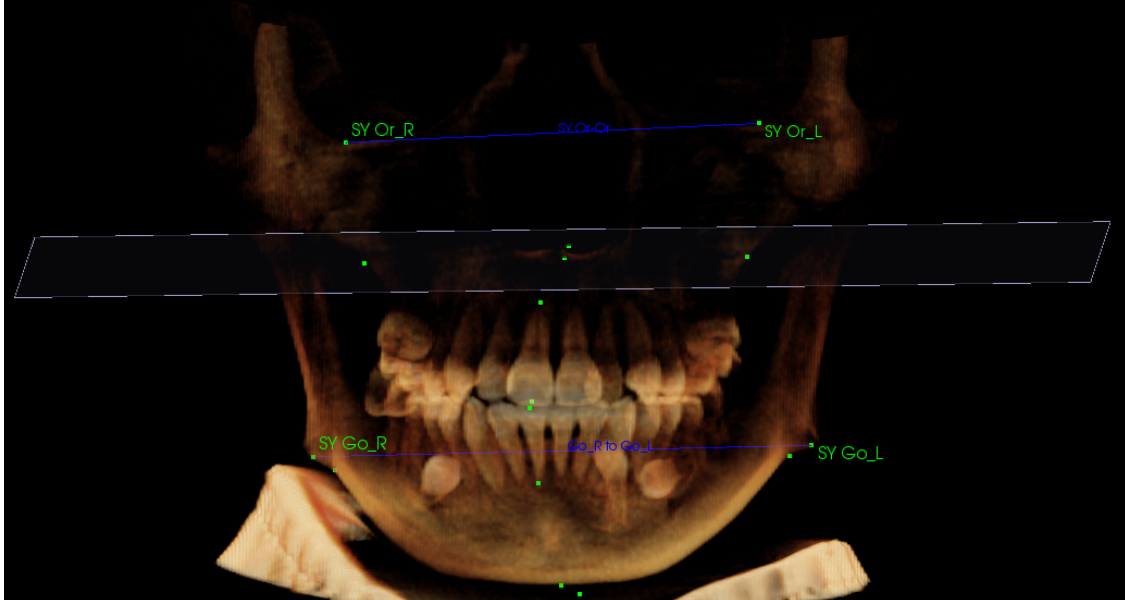
Figure 13: Frontal evaluation for transverse relationship or cants between cranial base, palatal plane or mandibular plane.

Overall, the analysis includes 9 measurements: 6 angular and 3 linear (Figure 14).

Table 2: Measurements from CBCT tracing

Measurements	Description
PP-MP	Angle between true palatal plane and mandibular plane in 3D
U1-PP	Angle between long axis of UR1 and palatal plane
L1-MP	Angle between long axis of LR1 and mandibular plane
Or-Or to PP	Cant between cranial base and palatal plane (degree)
PP to Go-Go	Cant between palatal plane and gonion-to-gonion line (degree)
Or-Or to Go-Go	Cant between cranial base and gonion-to-gonion line (degree)
Ag-Ag	Distance antegonial notches
J-point to J-point	Distance between J-points
Max trans deficiency	J-point to J-point + 10 - Ag-Ag

Figure 14: Sample of measurements from the analysis (Anatomage Invivo5).

Aim 3: To test the reliability of identifying 3D landmarks involved in palatal plane, mandibular plane, and associated measurements.

Inclusion criteria

5 subjects were chosen at random from patients who came to UCSF orthodontic clinic for beginning record between the dates of July 2013 to July 2015. Patients are in permanent dentition with all teeth erupted including second molars (DS4M2), Class I molar and canine relationship, and OB and OJ of 3mm or less.

Exclusion criteria

Subjects were excluded if they are missing any teeth besides third molars, have history of previous orthodontic treatment, or a diagnosis of craniofacial anomaly.

CBCT and lateral cephalograph

CBCTs and lateral cephalographs were taken by the same radiology technician on the same day of the visit. Size of the CBCT was 11x16cm and it did not include the cranial base.

Landmark identification

CBCT DICOM files were traced using the method described in Aim 2. Lateral cephalographs were imported and traced using Dolphin Imaging. Landmarks identified are as follow:

Menton, gonion, ANS, PNS, U1 tip, U1 root, L1 tip, L1 root, antegonial notch.

If there was a discrepancy between right and left side of the bilateral structure, examiner picked a point in between the two points (Figure 15).
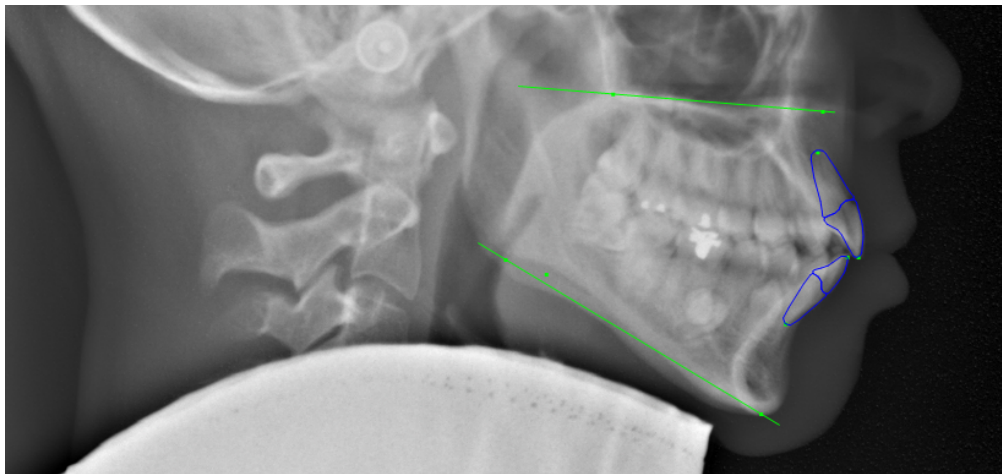
Figure 15: Discrepancy between right and left mandibular border.

The same examiner traced a set of 5 DICOM and 5 lateral cephalographs in random order, and then repeated an additional two rounds of tracing two weeks apart from each other. In total, there were 15 tracings of DICOM files and 15 tracings of lateral cephalographs.

Coordinates, centroids, and precision

For each 3D landmark traced, coordinates in three planes (x, y, z) were recorded. For each 2D landmark traced, coordinates in two planes (x, y) were recorded. In order to measure the reliability of each landmark's identification, deviation from average of all tracings on each

landmark was used. *Centroid* was defined as the average of all samples for a particular subject and landmark in each axis (Figure 16).
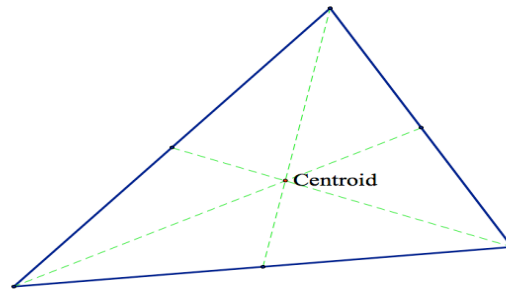
Figure 16: Centroid (depicted here in 2D) is the average point of the three points on the triangle.

Precision was defined as an average of deviations of points from centroid for a given landmark. Precision value was calculated in all three axes, then o*verall precision* was then calculated by combining all three axis using the Pythagorean Theorem. Smaller precision value indicates less deviation from average mark and, therefore, greater reliability of tracing the landmark.

Coordinates						Deviation				Centroid			Precision				
X	Y	Z	dX	dY	dZ	abs (dX)	abs (dY)	abs (dZ)	overall	Avg X	Avg Y	Avg Z	Avg dX	Avg dY	Avg dZ	Avg overall	SD
-3.10	-45.20	16.90	0.133	0.133	-0.133	0.133	0.133	0.133	0.231	-2.967	-45.067	16.767	0.089	1.178	0.244	**1.229**	0.868

Same steps were taken with 2D landmarks.

Coordinates				Deviation			Centroid		Precision			
Y	Z	dY	dZ	dY (abs)	dZ (abs)	overall	Avg Y	Avg Z	Avg dY	Avg dZ	Avg overall	SD
-22.900	-82.200	1.333	0.633	1.333	0.633	1.476	-21.567	-81.567	1.044	0.422	**1.219**	0.527

In order to compare the precision of 3D landmarks and 2D landmarks, precision values of 2D needed to be adjusted for the missing third dimension. This was accomplished by taking the square of 2D precision number, multiple by 1.5, then take a square root it.

Aim 4: To evaluate the difference between the palatal and mandibular plane associated measurements identified from the 3D CBCT analysis and 2D lateral cephalograph.

From both 3D CBCT tracing and 2D lateral cephalographs tracing, following measurements were recorded.

Palatal plane to mandibular plane angle (PP-MP).

Upper incisor to palatal angle (U1-PP).

Lower incisor to mandibular plane (L1-MP).

RESULTS

Aim 1: To study and compare the correlation between sella nasion-to-mandibular plane angle (SN-MP) to the palatal plane-to-mandibular plane angle (PP-MP), and open bite tendency.

There is a strong positive correlation, R= 0.859, between SN-MP and PP-MP (Figure 17). Both SN-MP and PP-MP have a negative correlation with overbite (Figure 17). However, correlation between PP-MP and overbite, R= -0.510, is a stronger one than between SN-MP and overbite, R= -0.479 (Figure 18, 19).
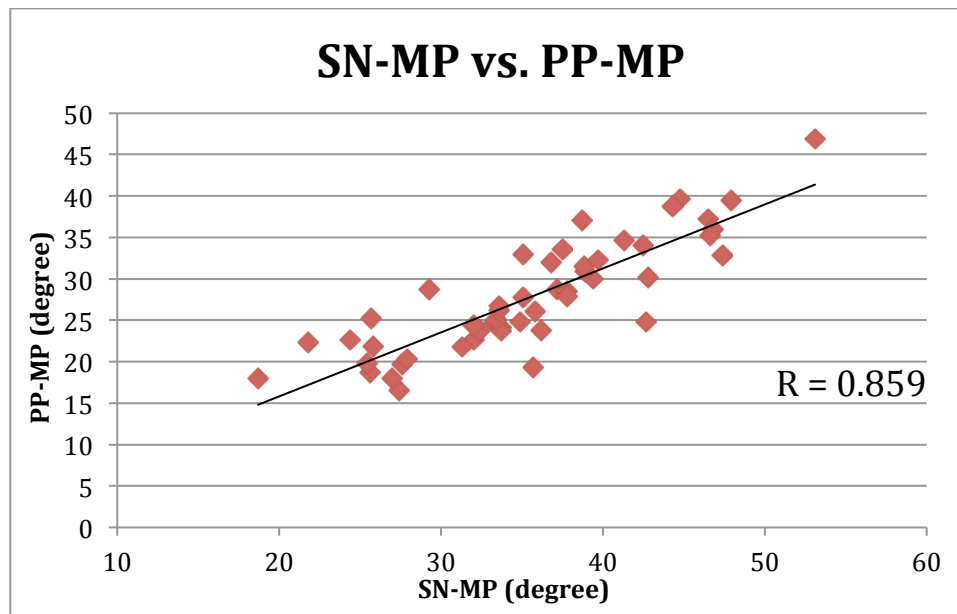
Figure 17: There is a strong positive correlation of R= 0.859 between SN-MP to PP-MP.
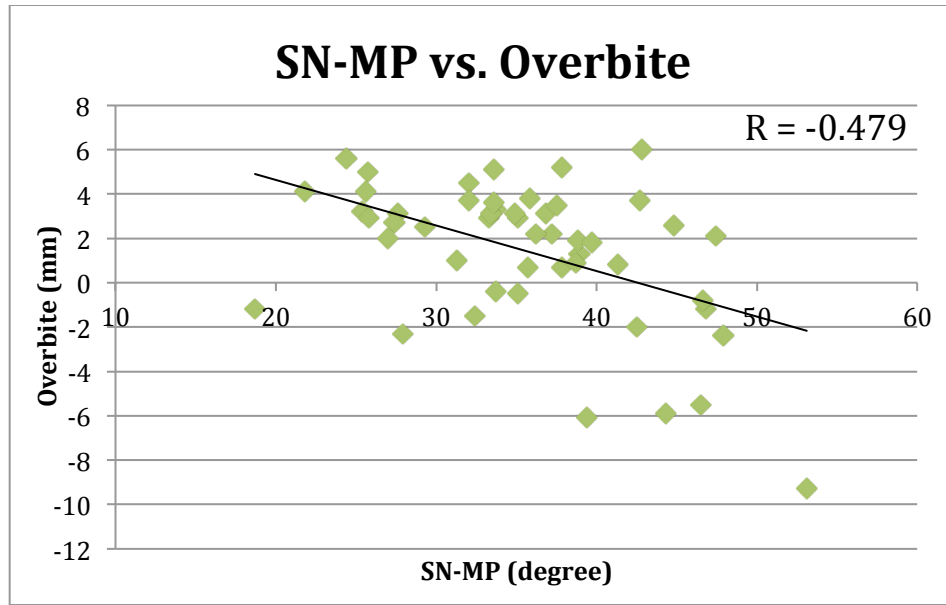
Figure 18: There is a negative correlation of R= -0.479 between SN-MP to overbite.
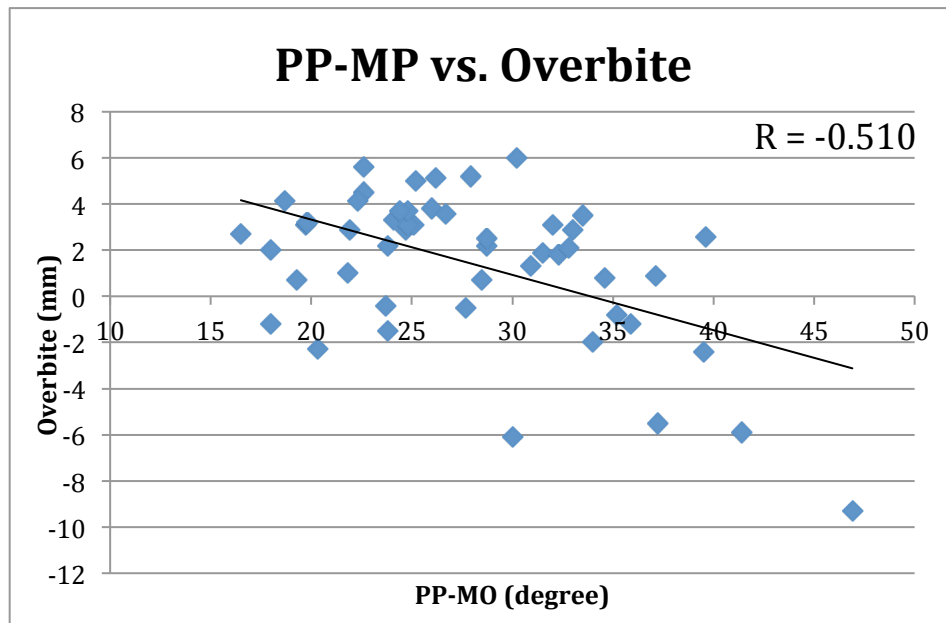
Figure 19: There is a negative correlation of R= -0.510 between PP-MP to overbite.

Aim 2: To develop method of identifying the palatal plane, mandibular plane, and associated landmarks in 3D on CBCT.

Aim 3: To test the reliability of 3D landmark identification involved in palatal plane, mandibular plane, and associated measurements.

Table 3: Precision of 3D tracing per subject

Subject #1

| Landmarks	Tracing #1				Tracing #2				Tracing #3				Overall				
	dX	dY	dZ	Precision	dX	dY	dZ	Precision	dX	dY	dZ	Precision	Avg dX	Avg dY	Avg dZ	Overall Precision	SD
ANS	0.000	0.167	0.200	0.260	0.000	0.133	0.000	0.133	0.000	0.033	0.200	0.203	0.000	0.111	0.133	0.199	0.064
PNS	1.100	0.100	0.133	1.113	0.800	0.100	0.033	0.807	1.900	0.200	0.167	1.918	1.267	0.133	0.111	1.279	0.574
J-point R	0.400	0.567	0.300	0.756	0.000	0.533	0.600	0.803	0.400	0.033	0.300	0.501	0.267	0.378	0.400	0.687	0.162
J-point L	0.233	0.067	0.067	0.252	0.067	0.467	0.333	0.577	0.167	0.533	0.267	0.619	0.156	0.356	0.222	0.483	0.201
Gonion R	0.067	0.100	0.033	0.125	0.133	0.100	0.267	0.314	0.067	0.000	0.233	0.243	0.089	0.067	0.178	0.227	0.096
AnteGn R	0.533	0.100	0.133	0.559	0.133	0.100	0.133	0.213	0.667	0.200	0.267	0.745	0.444	0.133	0.178	0.506	0.270
Me	0.800	0.133	0.033	0.812	0.700	0.167	0.267	0.767	0.100	0.033	0.233	0.256	0.533	0.111	0.178	0.612	0.309
Gonion L	0.300	0.100	0.100	0.332	0.300	0.100	0.000	0.316	0.600	0.200	0.100	0.640	0.400	0.133	0.067	0.429	0.183
AnteGn L	0.000	0.033	0.167	0.170	0.100	0.067	0.033	0.125	0.100	0.033	0.133	0.170	0.067	0.044	0.111	0.155	0.026
UR1 Crown	0.000	0.100	0.067	0.120	0.100	0.100	0.133	0.194	0.100	0.000	0.067	0.120	0.067	0.067	0.089	0.145	0.043
UR1 Root	0.033	0.100	0.000	0.105	0.067	0.100	0.000	0.120	0.033	0.000	0.000	0.033	0.044	0.067	0.000	0.086	0.046
LR1 Root	1.133	0.033	0.267	1.165	0.733	0.133	0.133	0.757	1.867	0.167	0.133	1.879	1.244	0.111	0.178	1.267	0.568
LR1 Crown	0.167	0.033	0.000	0.170	0.067	0.067	0.200	0.221	0.233	0.033	0.200	0.309	0.156	0.044	0.133	0.233	0.070
Orbital L	0.367	0.100	0.600	0.710	0.033	0.000	0.000	0.033	0.333	0.100	0.600	0.694	0.244	0.067	0.400	0.479	0.386
Orbital R	0.167	0.067	0.267	0.321	0.533	0.033	0.733	0.907	0.367	0.033	0.467	0.594	0.356	0.044	0.489	0.608	0.293
Average	0.353	0.120	0.158	0.465	0.251	0.147	0.191	0.419	0.462	0.107	0.224	0.595	0.356	0.124	0.191	0.493	0.370

Subject #2

Landmarks	Tracing #1				Tracing #2				Tracing #3				Overall				
	dX	dY	dZ	Precision	dX	dY	dZ	Precision	dX	dY	dZ	Precision	Avg dX	Avg dY	Avg dZ	Overall Precision	SD
ANS	1.900	0.177	0.333	1.937	1.200	0.077	0.033	1.203	0.700	0.253	0.367	0.830	1.267	0.169	0.244	1.323	0.563
PNS	0.033	0.567	0.333	0.658	0.467	0.133	0.167	0.513	0.433	0.433	0.167	0.635	0.311	0.378	0.222	0.602	0.078
J-point R	0.333	0.533	0.467	0.783	0.367	0.467	0.233	0.638	0.033	0.067	0.233	0.245	0.244	0.356	0.311	0.555	0.278
J-point L	0.067	0.433	0.133	0.458	0.333	0.067	0.233	0.412	0.267	0.367	0.367	0.583	0.222	0.289	0.244	0.485	0.088
Gonion R	0.633	0.133	0.133	0.661	1.267	0.367	0.267	1.345	0.633	0.233	0.133	0.688	0.844	0.244	0.178	0.898	0.388
AnteGn R	0.267	0.000	0.433	0.509	0.067	0.100	0.167	0.205	0.333	0.100	0.267	0.438	0.222	0.067	0.289	0.384	0.159
Me	0.133	0.233	0.367	0.455	0.467	0.167	0.233	0.548	0.333	0.067	0.133	0.365	0.311	0.156	0.244	0.456	0.091
Gonion L	0.533	0.067	0.367	0.651	0.167	0.033	0.133	0.216	0.367	0.033	0.233	0.436	0.356	0.044	0.244	0.434	0.217
AnteGn L	0.600	0.167	0.467	0.778	1.200	0.333	0.433	1.319	0.600	0.167	0.033	0.624	0.800	0.222	0.311	0.907	0.365
UR1 Crown	0.033	0.100	0.467	0.478	0.067	0.100	0.233	0.262	0.033	0.200	0.233	0.309	0.044	0.133	0.311	0.350	0.114
UR1 Root	0.000	0.233	0.033	0.236	0.200	0.033	0.033	0.205	0.200	0.267	0.067	0.340	0.133	0.178	0.044	0.260	0.071
LR1 Root	0.233	0.167	0.100	0.304	0.267	0.333	0.200	0.471	0.033	0.167	0.100	0.197	0.178	0.222	0.133	0.324	0.138
LR1 Crown	0.033	0.033	0.100	0.111	0.033	0.067	0.100	0.125	0.067	0.033	0.200	0.213	0.044	0.044	0.133	0.150	0.056
Orbital L	0.067	0.133	0.000	0.149	0.067	0.033	0.000	0.075	0.133	0.167	0.000	0.213	0.089	0.111	0.000	0.146	0.070
Orbital R	0.033	0.067	0.003	0.075	0.267	0.033	0.197	0.333	0.233	0.033	0.193	0.305	0.178	0.044	0.131	0.237	0.142
Average	0.327	0.203	0.249	0.549	0.429	0.156	0.178	0.525	0.293	0.172	0.182	0.428	0.350	0.177	0.203	0.501	0.323

Subject #3

Landmarks	Tracing #1				Tracing #2				Tracing #3				Overall				
	dX	dY	dZ	Precision	dX	dY	dZ	Precision	dX	dY	dZ	Precision	Avg dX	Avg dY	Avg dZ	Overall Precision	SD
ANS	0.600	0.233	0.067	0.647	0.500	0.367	0.067	0.624	0.100	0.133	0.133	0.213	0.400	0.244	0.089	0.495	0.244
PNS	0.400	0.067	0.367	0.547	0.300	0.167	0.033	0.345	0.100	0.233	0.333	0.419	0.267	0.156	0.244	0.437	0.102
J-point R	0.633	0.300	0.533	0.881	0.767	0.100	0.267	0.818	0.133	0.400	0.267	0.499	0.511	0.267	0.356	0.732	0.205
J-point L	1.267	0.533	0.333	1.414	0.433	0.167	0.267	0.535	0.833	0.367	0.067	0.913	0.844	0.356	0.222	0.954	0.441
Gonion R	0.200	0.067	0.167	0.269	0.000	0.067	0.267	0.275	0.200	0.133	0.433	0.496	0.133	0.089	0.289	0.346	0.129
AnteGn R	0.267	0.100	0.233	0.368	0.533	0.100	0.167	0.568	0.267	0.200	0.067	0.340	0.356	0.133	0.156	0.425	0.124
Me	0.433	0.100	0.700	0.829	0.033	0.500	0.100	0.511	0.467	0.400	0.600	0.859	0.311	0.333	0.467	0.733	0.193
Gonion L	1.267	0.533	0.700	1.542	0.133	0.167	0.000	0.213	1.133	0.367	0.700	1.382	0.844	0.356	0.467	1.046	0.725
AnteGn L	0.867	0.033	0.600	1.055	0.733	0.067	0.800	1.087	0.133	0.033	1.400	1.407	0.578	0.044	0.933	1.183	0.195
UR1 Crown	0.267	0.067	0.167	0.321	0.033	0.033	0.033	0.058	0.233	0.033	0.133	0.271	0.178	0.044	0.111	0.217	0.140
UR1 Root	0.067	0.267	0.000	0.275	0.033	0.067	0.100	0.125	0.033	0.333	0.100	0.350	0.044	0.222	0.067	0.250	0.115
LR1 Root	0.067	0.033	0.133	0.153	0.033	0.233	0.067	0.245	0.033	0.267	0.067	0.277	0.044	0.178	0.089	0.225	0.064
LR1 Crown	0.033	0.167	0.200	0.262	0.033	0.133	0.300	0.330	0.067	0.033	0.100	0.125	0.044	0.111	0.200	0.239	0.105
Orbital L	0.200	0.233	0.067	0.314	0.000	0.233	0.133	0.269	0.200	0.467	0.067	0.512	0.133	0.311	0.089	0.365	0.129
Orbital R	0.333	0.167	0.300	0.478	0.367	0.067	0.700	0.793	0.033	0.233	1.000	1.027	0.244	0.156	0.667	0.766	0.275
Average	0.460	0.193	0.304	0.624	0.262	0.164	0.220	0.453	0.264	0.242	0.364	0.606	0.329	0.200	0.296	0.561	0.320

Subject #4

Landmarks	Tracing #1				Tracing #2				Tracing #3				Overall				
	dX	dY	dZ	Precision	dX	dY	dZ	Precision	dX	dY	dZ	Precision	Avg dX	Avg dY	Avg dZ	Overall Precision	SD
ANS	0.133	0.133	0.467	0.503	0.367	0.067	0.067	0.379	0.233	0.067	0.533	0.586	0.244	0.089	0.356	0.489	0.104
PNS	1.867	0.300	0.067	1.892	1.233	0.000	0.033	1.234	0.633	0.300	0.033	0.702	1.244	0.200	0.044	1.276	0.596
J-point R	0.467	0.533	0.533	0.887	0.067	0.467	0.467	0.663	0.533	0.067	0.067	0.542	0.356	0.356	0.356	0.697	0.175
J-point L	1.300	0.167	0.167	1.321	0.100	0.267	0.067	0.292	1.400	0.433	0.233	1.484	0.933	0.289	0.156	1.033	0.646
Gonion R	0.633	0.333	0.300	0.776	0.733	0.233	0.000	0.770	1.367	0.567	0.300	1.510	0.911	0.378	0.200	1.018	0.425
AnteGn R	0.867	0.167	0.433	0.983	1.033	0.333	0.767	1.329	0.167	0.167	0.333	0.408	0.689	0.222	0.511	0.907	0.465
Me	0.133	0.167	0.000	0.213	0.067	0.067	0.100	0.137	0.067	0.233	0.100	0.262	0.089	0.156	0.067	0.204	0.063
Gonion L	0.567	0.033	0.200	0.602	0.667	0.233	0.400	0.812	1.233	0.267	0.600	1.397	0.822	0.178	0.400	0.937	0.412
AnteGn L	0.333	0.000	0.233	0.407	0.267	0.100	0.133	0.314	0.067	0.100	0.367	0.386	0.222	0.067	0.244	0.369	0.048
UR1 Crown	0.033	0.033	0.100	0.111	0.067	0.067	0.200	0.221	0.033	0.033	0.100	0.111	0.044	0.044	0.133	0.147	0.064
UR1 Root	0.167	0.233	0.267	0.392	0.067	0.067	0.067	0.115	0.233	0.167	0.333	0.440	0.156	0.156	0.222	0.316	0.175
LR1 Root	0.167	0.233	0.200	0.350	0.233	0.167	0.000	0.287	0.067	0.067	0.200	0.221	0.156	0.156	0.133	0.286	0.064
LR1 Crown	0.167	0.133	0.067	0.224	0.033	0.067	0.267	0.277	0.133	0.067	0.333	0.365	0.111	0.089	0.222	0.289	0.071
Orbital L	0.233	0.000	0.200	0.307	0.467	0.000	0.600	0.760	0.233	0.000	0.800	0.833	0.311	0.000	0.533	0.634	0.285
Orbital R	0.033	0.167	0.200	0.262	0.333	0.133	0.600	0.699	0.367	0.033	0.400	0.544	0.244	0.111	0.400	0.502	0.221
Average	0.473	0.176	0.229	0.615	0.382	0.151	0.251	0.553	0.451	0.171	0.316	0.653	0.436	0.166	0.265	0.607	0.354

Subject #5	Tracing #1				Tracing #2				Tracing #3				Overall				
Landmarks	dX	dY	dZ	Precision	dX	dY	dZ	Precision	dX	dY	dZ	Precision	Avg dX	Avg dY	Avg dZ	Overall Precision	SD
ANS	1.100	0.200	0.433	1.199	1.700	0.000	0.933	1.939	2.800	0.200	1.367	3.122	1.867	0.133	0.911	2.087	0.970
PNS	0.267	0.000	0.033	0.269	1.133	0.200	0.067	1.153	0.867	0.200	0.033	0.890	0.756	0.133	0.044	0.771	0.454
J-point R	0.333	0.633	0.267	0.764	0.233	0.233	0.467	0.572	0.567	0.867	0.733	1.269	0.378	0.578	0.489	0.868	0.360
J-point L	0.533	0.433	0.633	0.935	0.267	0.667	0.367	0.806	0.267	0.233	0.267	0.443	0.356	0.444	0.422	0.728	0.255
Gonion R	0.133	0.167	0.167	0.271	0.033	0.133	0.067	0.153	0.167	0.033	0.233	0.289	0.111	0.111	0.156	0.237	0.074
AnteGn R	0.200	0.033	0.033	0.205	0.200	0.067	0.133	0.249	0.400	0.033	0.167	0.435	0.267	0.044	0.111	0.297	0.122
Me	0.267	0.200	0.133	0.359	0.033	0.000	0.467	0.468	0.233	0.200	0.333	0.453	0.178	0.133	0.311	0.427	0.059
Gonion L	0.533	0.033	0.033	0.535	0.167	0.067	0.167	0.245	0.367	0.033	0.133	0.392	0.356	0.044	0.111	0.391	0.145
AnteGn L	0.100	0.200	0.267	0.348	0.000	0.100	0.167	0.194	0.100	0.100	0.433	0.456	0.067	0.133	0.289	0.333	0.131
UR1 Crown	0.100	0.100	0.400	0.424	0.100	0.000	0.100	0.141	0.000	0.100	0.300	0.316	0.067	0.067	0.267	0.294	0.143
UR1 Root	0.100	0.100	0.167	0.219	0.300	0.100	0.167	0.357	0.200	0.200	0.333	0.437	0.200	0.133	0.222	0.338	0.111
LR1 Root	0.167	0.267	0.067	0.321	0.033	0.033	0.033	0.058	0.133	0.233	0.033	0.271	0.111	0.178	0.044	0.217	0.140
LR1 Crown	0.067	0.067	0.000	0.094	0.033	0.233	0.200	0.309	0.033	0.167	0.200	0.262	0.044	0.156	0.133	0.222	0.113
Orbital L	0.333	0.167	0.733	0.823	0.167	0.033	0.267	0.316	0.167	0.133	0.467	0.513	0.222	0.111	0.489	0.551	0.255
Orbital R	0.767	0.233	1.067	1.334	0.333	0.067	0.433	0.551	0.433	0.167	0.633	0.785	0.511	0.156	0.711	0.890	0.402
Average	0.333	0.189	0.296	0.540	0.316	0.129	0.269	0.501	0.449	0.193	0.378	0.689	0.366	0.170	0.314	0.577	0.480

Table 4: Precision of 2D tracing per subject

Subject #1

Landmarks	Tracing #1				Tracing #2				Tracing #3				Overall				
	dX	dY	Precision	Adjusted	dX	dY	Precision	Adjusted	dX	dY	Precision	Adjusted	dX	dY	Precision	Adjusted Precision	SD
ANS	0.033	1.567	1.567	1.919	0.333	1.733	1.765	2.162	0.367	0.167	0.403	0.493	0.244	1.156	1.245	1.525	0.901
AnteGn	0.633	1.567	1.690	2.070	0.333	1.133	1.181	1.447	0.967	0.433	1.059	1.297	0.644	1.044	1.310	1.605	0.410
Gonion	0.700	1.067	1.276	1.563	1.200	0.633	1.357	1.662	0.500	0.433	0.662	0.810	0.800	0.711	1.098	1.345	0.466
LR1 root	0.600	0.067	0.604	0.739	0.700	1.033	1.248	1.529	0.100	0.967	0.972	1.190	0.467	0.689	0.941	1.153	0.396
LR1 crown	0.100	0.900	0.906	1.109	0.000	0.900	0.900	1.102	0.100	0.000	0.100	0.122	0.067	0.600	0.635	0.778	0.568
Menton	0.500	0.833	0.972	1.190	0.000	1.267	1.267	1.551	0.500	0.433	0.662	0.810	0.333	0.844	0.967	1.184	0.371
PNS	2.000	0.467	2.054	2.515	1.000	0.533	1.133	1.388	1.000	0.067	1.002	1.227	1.333	0.356	1.396	1.710	0.702
UR1 root	0.100	1.567	1.570	1.923	0.400	0.633	0.749	0.917	0.500	0.933	1.059	1.297	0.333	1.044	1.126	1.379	0.508
UR1 crown	0.100	0.767	0.773	0.947	0.000	1.333	1.333	1.633	0.100	0.567	0.575	0.705	0.067	0.889	0.894	1.095	0.481
Average	0.530	0.978	1.268	1.553	0.441	1.022	1.215	1.488	0.459	0.444	0.722	0.884	0.477	0.815	1.068	1.308	0.534

Subject #2

Landmarks	Tracing #1				Tracing #2				Tracing #3				Overall				
	dX	dY	Precision	Adjusted	dX	dY	Precision	Adjusted	dX	dY	Precision	Adjusted	dX	dY	Precision	Adjusted Precision	SD
ANS	1.200	0.600	1.342	1.643	1.300	0.500	1.393	1.706	0.100	0.100	0.141	0.173	0.867	0.400	0.959	1.174	0.867
AnteGn	1.633	0.567	1.729	2.117	0.433	1.433	1.497	1.834	2.067	0.867	2.241	2.745	1.378	0.956	1.822	2.232	0.466
Gonion	2.533	0.267	2.547	3.120	1.167	1.133	1.627	1.992	1.367	0.867	1.618	1.982	1.689	0.756	1.931	2.365	0.654
LR1 root	1.367	1.733	2.207	2.703	0.833	1.267	1.516	1.857	0.533	0.467	0.709	0.868	0.911	1.156	1.477	1.809	0.919
LR1 crown	0.133	0.933	0.943	1.155	0.067	1.067	1.069	1.309	0.067	0.133	0.149	0.183	0.089	0.711	0.720	0.882	0.611
Menton	0.333	1.733	1.765	2.162	0.233	1.267	1.288	1.577	0.567	0.467	0.734	0.899	0.378	1.156	1.262	1.546	0.632
PNS	0.733	0.733	1.037	1.270	0.533	0.467	0.709	0.868	1.267	0.267	1.294	1.585	0.844	0.489	1.013	1.241	0.360
UR1 root	0.967	0.000	0.967	1.184	0.333	0.800	0.867	1.061	0.633	0.800	1.020	1.250	0.644	0.533	0.951	1.165	0.096
UR1 crown	0.467	0.933	1.043	1.278	0.533	1.067	1.193	1.461	0.067	0.133	0.149	0.183	0.356	0.711	0.795	0.974	0.691
Average	1.041	0.833	1.509	1.848	0.604	1.000	1.240	1.518	0.741	0.456	0.895	1.096	0.795	0.763	1.215	1.488	0.588

Subject #3

Landmarks	Tracing #1				Tracing #2				Tracing #3				Overall				
	dX	dY	Precision	Adjusted	dX	dY	Precision	Adjusted	dX	dY	Precision	Adjusted	dX	dY	Precision	Adjusted Precision	SD
ANS	1.000	1.233	1.588	1.945	0.200	0.233	0.307	0.376	1.200	1.467	1.895	2.321	0.800	0.978	1.263	1.547	1.031
AnteGn	1.500	0.733	1.670	2.045	0.300	0.933	0.980	1.201	1.200	1.667	2.054	2.515	1.000	1.111	1.568	1.920	0.666
Gonion	0.067	1.500	1.501	1.839	1.233	0.300	1.269	1.555	1.167	1.800	2.145	2.627	0.822	1.200	1.639	2.007	0.556
LR1 root	0.567	0.400	0.694	0.850	1.133	1.400	1.801	2.206	0.567	1.800	1.887	2.311	0.756	1.200	1.461	1.789	0.815
LR1 crown	0.000	0.167	0.167	0.204	0.500	1.167	1.269	1.555	0.500	1.333	1.424	1.744	0.333	0.889	0.953	1.168	0.840
Menton	0.767	0.900	1.182	1.448	0.067	1.200	1.202	1.472	0.833	2.100	2.259	2.767	0.556	1.400	1.548	1.896	0.755
PNS	0.467	0.633	0.787	0.964	0.333	0.833	0.898	1.099	0.133	1.467	1.473	1.804	0.311	0.978	1.052	1.289	0.451
UR1 root	0.000	3.533	3.533	4.327	0.200	3.467	3.472	4.253	0.200	0.067	0.211	0.258	0.133	2.356	2.406	2.946	2.328
UR1 crown	0.033	0.767	0.767	0.940	0.467	0.767	0.898	1.099	0.433	1.533	1.593	1.951	0.311	1.022	1.086	1.330	0.544
Average	0.489	1.096	1.321	1.618	0.493	1.144	1.344	1.646	0.693	1.470	1.660	2.033	0.558	1.237	1.442	1.766	0.887

Subject #4

Landmarks	Tracing #1				Tracing #2				Tracing #3				Overall				
	dX	dY	Precision	Adjusted	dX	dY	Precision	Adjusted	dX	dY	Precision	Adjusted	dX	dY	Precision	Adjusted Precision	SD
ANS	0.433	0.433	0.613	0.751	0.067	0.833	0.836	1.024	0.367	1.267	1.319	1.615	0.289	0.844	0.922	1.130	0.442
AnteGn	0.900	0.167	0.915	1.121	1.000	0.167	1.014	1.242	0.100	0.333	0.348	0.426	0.667	0.222	0.759	0.930	0.440
Gonion	1.967	0.900	2.163	2.649	1.233	0.400	1.297	1.588	0.733	1.300	1.493	1.828	1.311	0.867	1.651	2.022	0.556
LR1 root	0.433	0.133	0.453	0.555	1.367	2.167	2.562	3.137	0.933	2.033	2.237	2.740	0.911	1.444	1.751	2.144	1.390
LR1 crown	0.333	0.067	0.340	0.416	0.167	0.833	0.850	1.041	0.167	0.767	0.785	0.961	0.222	0.556	0.658	0.806	0.340
Menton	0.067	0.033	0.075	0.091	0.433	0.867	0.969	1.187	0.367	0.833	0.910	1.115	0.289	0.578	0.651	0.798	0.613
PNS	5.633	0.400	5.648	6.917	2.867	0.800	2.976	3.645	2.767	0.400	2.795	3.424	3.756	0.533	3.806	4.662	1.956
UR1 root	0.900	0.667	1.120	1.372	0.800	0.667	1.041	1.275	0.100	1.333	1.337	1.638	0.600	0.889	1.166	1.428	0.188
UR1 crown	0.033	0.233	0.236	0.289	0.067	0.667	0.670	0.821	0.033	0.433	0.435	0.532	0.044	0.444	0.447	0.547	0.266
Average	1.189	0.337	1.285	1.573	0.889	0.822	1.357	1.662	0.619	0.967	1.295	1.587	0.899	0.709	1.312	1.607	0.688

Subject #5

Landmarks	Tracing #1				Tracing #2				Tracing #3				Overall				
	dX	dY	Precision	Adjusted	dX	dY	Precision	Adjusted	dX	dY	Precision	Adjusted	dX	dY	Precision	Adjusted Precision	SD
ANS	1.567	0.067	1.568	1.921	0.233	0.567	0.613	0.751	1.333	0.633	1.476	1.808	1.044	0.422	1.219	1.493	0.645
AnteGn	0.233	0.367	0.435	0.532	0.667	0.067	0.670	0.821	0.433	0.433	0.613	0.751	0.444	0.289	0.572	0.701	0.150
Gonion	0.400	0.900	0.985	1.206	0.200	1.300	1.315	1.611	0.200	0.400	0.447	0.548	0.267	0.867	0.916	1.122	0.537
LR1 root	0.433	1.000	1.090	1.335	0.633	1.000	1.184	1.450	1.067	0.000	1.067	1.306	0.711	0.667	1.113	1.364	0.076
LR1 crown	0.267	0.267	0.377	0.462	0.333	0.833	0.898	1.099	0.067	0.567	0.571	0.699	0.222	0.556	0.615	0.753	0.322
Menton	1.433	0.800	1.641	2.010	0.867	1.100	1.400	1.715	0.567	0.300	0.641	0.785	0.956	0.733	1.228	1.504	0.639
PNS	0.100	0.567	0.575	0.705	0.300	0.733	0.792	0.970	0.200	0.167	0.260	0.319	0.200	0.489	0.543	0.665	0.328
UR1 root	0.367	0.833	0.910	1.115	0.433	0.667	0.795	0.974	0.067	0.167	0.180	0.220	0.289	0.556	0.628	0.770	0.481
UR1 crown	0.067	1.000	1.002	1.227	0.133	1.100	1.108	1.357	0.067	0.100	0.120	0.147	0.089	0.733	0.743	0.911	0.664
Average	0.541	0.644	0.954	1.168	0.422	0.819	0.975	1.194	0.444	0.307	0.597	0.731	0.469	0.590	0.842	1.031	0.427

X-axis represents coordinates in anterior-posterior direction, Y-axis represents coordinates in superior-inferior direction, and Z-axis represents coordinates in subjects' right and left (Figure 20). In order to compare precision of 3D and 2D tracing, the overall precision of 2D tracing was adjusted for the missing the third plane.
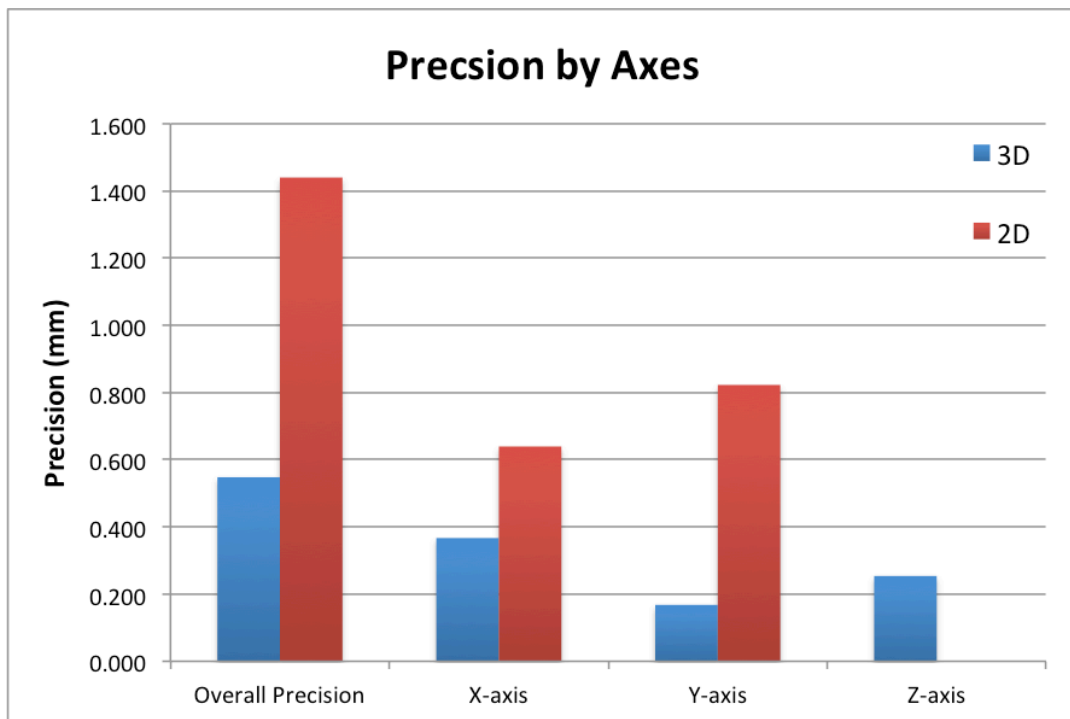

Figure 20: Precision of 3D tracing and 2D tracing by axes.

Table 5: Precision by landmarks

| Landmark	3D Precision	3D SD	2D Precision	2D SD	Unpaired T-test P-value
LR1 Crown	0.227	0.086	0.877	0.506	<0.0001
UR1 Crown	0.231	0.124	0.971	0.536	<0.0001
UR1 Root	0.250	0.132	1.538	1.200	<0.001
LR1 Root	0.464	0.477	1.652	0.805	<0.0001
Menton	0.486	0.236	1.385	0.646	<0.0001
AnteGn R	0.504	0.312	1.478	0.714	<0.0001
Gonion R	0.546	0.421	1.772	0.672	<0.0001
AnteGn L	0.589	0.435	1.478	0.714	<0.001
Gonion L	0.647	0.447	1.772	0.672	<0.0001
PNS	0.873	0.508	1.913	1.680	<0.05
ANS	0.919	0.841	1.374	0.706	0.120
Average	0.548	0.351	1.440	0.829	<0.0001
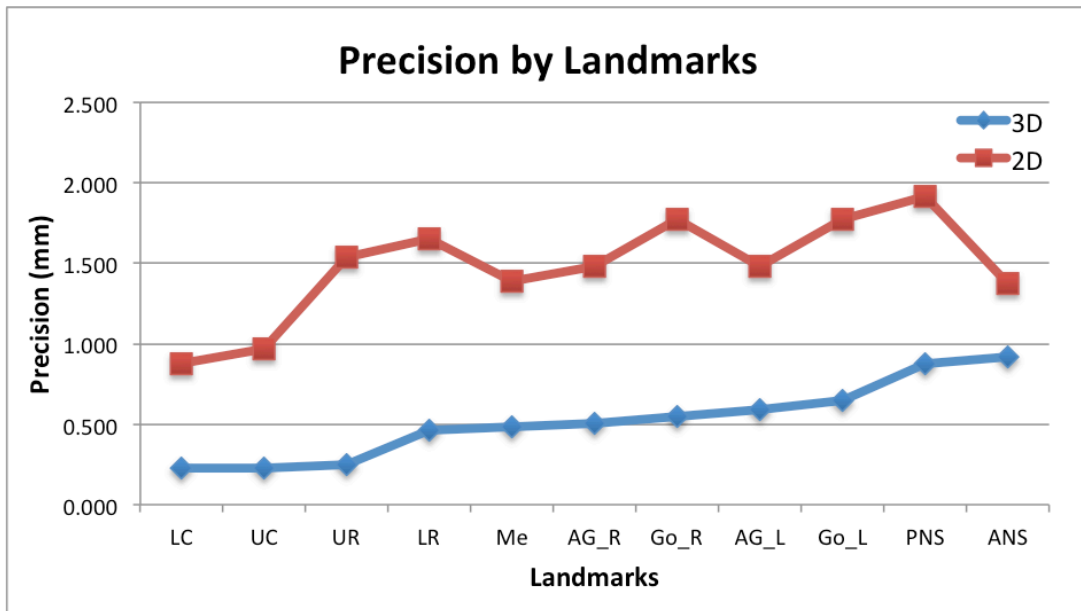
Figure 21: Precision of 3D tracing and 2D tracing by landmarks.

The precision of 3D tracing was greater than that of 2D tracing for all of the landmarks evaluated (Figure 21).

Table 6: Overall precision and ranking of landmarks in 3D tracing.

Ranking	Landmark	Overall Precision	X-axis	Y-axis	Z-axis	SD
1	LR1 Crown	0.227	0.080	0.089	0.164	0.086
2	UR1 Crown	0.231	0.080	0.071	0.182	0.124
3	UR1 Root	0.250	0.116	0.151	0.111	0.132
4	Orbital L	0.435	0.200	0.120	0.302	0.276
5	LR1 Root	0.464	0.347	0.169	0.116	0.477
6	Menton	0.486	0.284	0.178	0.253	0.236
7	AnteGn R	0.504	0.396	0.120	0.249	0.312
8	Gonion R	0.546	0.418	0.178	0.200	0.421
9	AnteGn L	0.589	0.347	0.102	0.378	0.435
10	Orbital R	0.601	0.307	0.102	0.480	0.332
11	Gonion L	0.647	0.556	0.151	0.258	0.447
12	J-point R	0.708	0.351	0.387	0.382	0.233
13	J-point L	0.736	0.502	0.347	0.253	0.400
14	PNS	0.873	0.769	0.200	0.133	0.508
15	ANS	0.919	0.756	0.149	0.347	0.841
-	Average	0.548	0.367	0.168	0.254	0.351

Table 7: Overall precision and ranking of landmarks in 2D tracing.

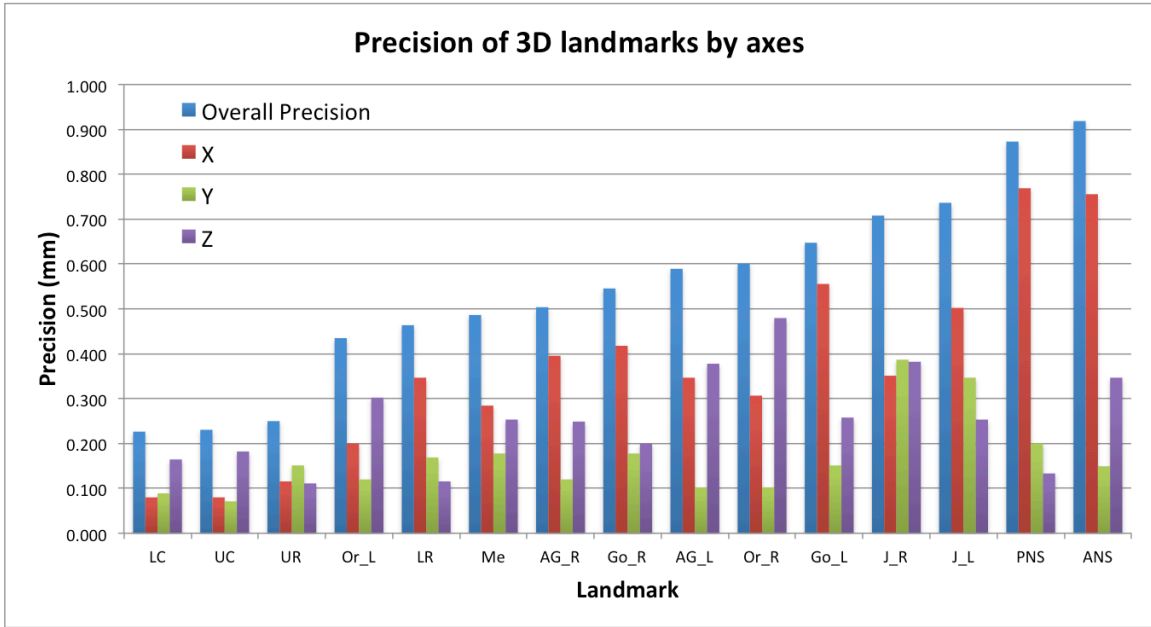| Ranking	Landmark	Overall Precision	Avg dX	Avg dY	SD
1	LR1 Crown	0.877	0.187	0.662	0.506
2	UR1 Crown	0.971	0.173	0.760	0.536
3	ANS	1.374	0.649	0.760	0.706
4	Menton	1.385	0.502	0.942	0.646
5	AnteGn	1.478	0.827	0.724	0.714
6	UR1 Root	1.538	0.400	1.076	1.200
7	LR1 Root	1.652	0.751	1.031	0.805
8	Gonion	1.772	0.978	0.880	0.672
9	PNS	1.913	1.289	0.569	1.680
-	Average	1.440	0.640	0.823	0.829

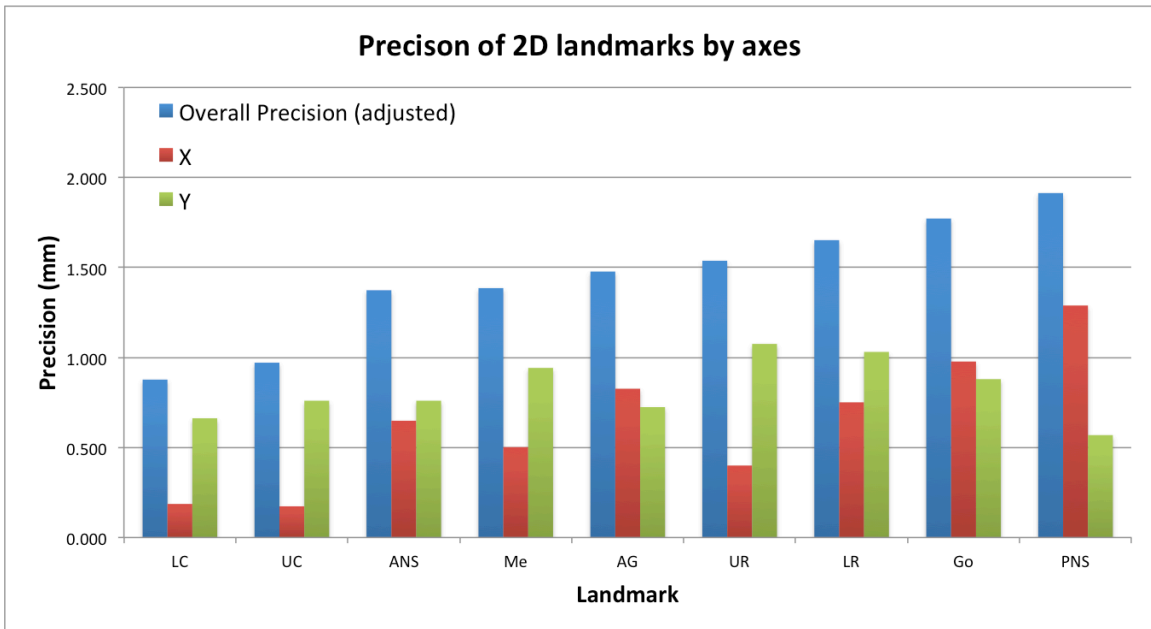Figure 22: Precision of 3D landmarks tracing by axes.

Figure 23: Precision of 2D landmarks tracing by axes.

Aim 4: To evaluate the difference between the palatal and mandibular planes' associated measurements identified from the 3D CBCT analysis and 2D lateral cephalograph.
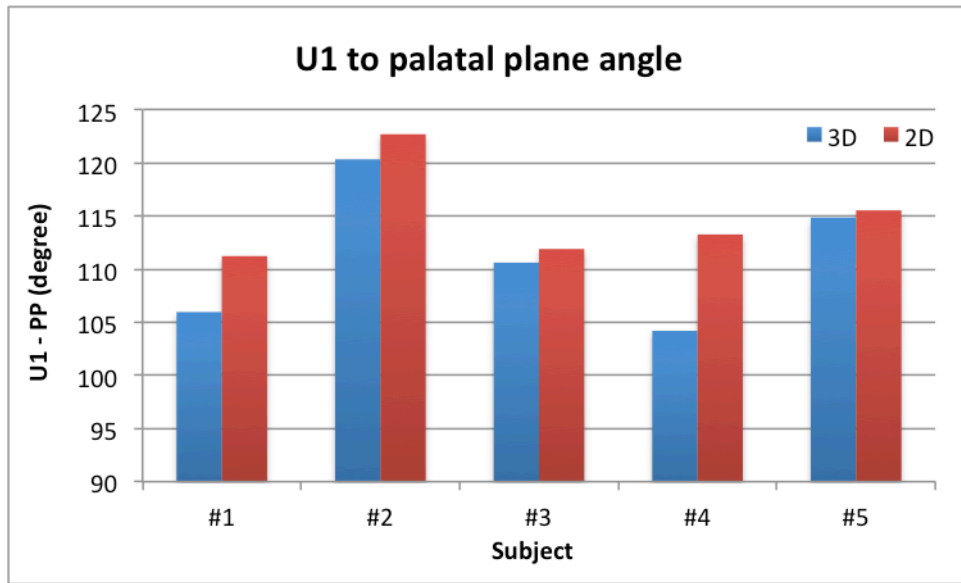

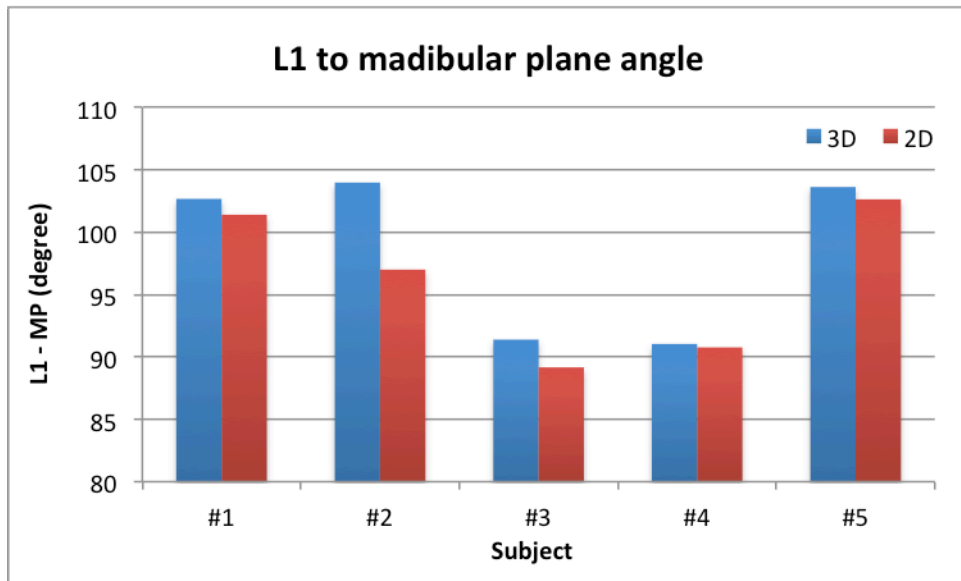Figure 24: Comparison of U1-palatal plane angle between 3D and 2D tracing.

Figure 25: Comparison of L1-mandibular plane angle between 3D and 2D tracing.
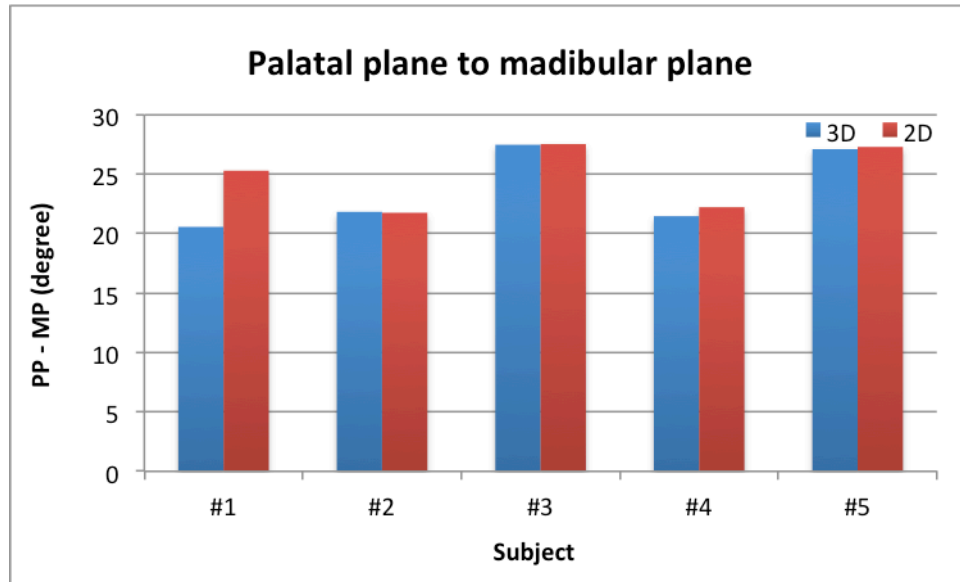
Figure 26: Comparison of palatal plane-to-mandibular angle between 3D and 2D tracing.

Table 8: Wilcoxon signed rank test to compare three measurements, U1-PP, L1-MP, PP-MP, between 3D and 2D tracing of given subjects.

Subject - Tracing	U1-PP (3D)	U1-PP (2D)	L1-MP (3D)	L1-MP (2D)	PP-MP (3D)	PP-MP (2D)
1-1	106.66	112.60	102.55	101.60	19.84	24.40
1-2	106.21	109.70	103.01	103.20	20.64	26.40
1-3	105.03	111.40	102.46	99.40	21.16	25.00
2-1	121.10	122.60	103.30	95.30	21.51	21.80
2-2	119.78	122.10	104.14	98.80	21.93	21.20
2-3	120.14	123.40	104.49	96.90	21.99	22.20
3-1	109.77	114.10	93.10	87.40	27.43	26.60
3-2	111.01	108.70	93.83	90.40	26.59	28.50
3-3	111.06	112.90	87.25	89.70	28.32	27.40
4-1	104.49	114.80	92.43	90.90	21.54	23.50
4-2	104.01	112.50	92.99	89.30	21.66	22.00
4-3	104.09	112.50	87.71	92.10	21.14	21.10
5-1	115.26	113.70	103.79	102.40	26.52	28.50
5-2	116.60	117.00	103.47	103.90	26.19	26.90
5-3	112.72	115.90	103.61	101.60	28.51	26.40
Avg difference (3D-2D)	-3.73		2.35		-1.13	
Wilcoxon's W	8		21		34	
P-value	**0.001 < P < 0.005**		**0.02 < P < 0.05**		0.10 < P < 0.20	

DISCUSSION

Aim 1

The strong correlation, R=0.859, between sella nasion-to-mandibular plane angle (SN-MP) and the palatal plane-to-mandibular plane angle (PP-MP) shows that PP-MP can be used to predict trend of SN-MP and vertical jaw relationship when SN-MP is not available. A commonly used reset or progress CBCT, 10x10, and beginning or final record CBCT with limited field of view, 11x17, are examples of this type of scan used to do this analysis. In these radiographs, the cranial base is excluded in order to minimize the field of view and lower the patient's exposure to radiation.

PP-MP and overbite have very similar relationship to SN-MP and overbite. The R value is actually stronger between PP-MP and overbite (R= -0.510) than between SN-MP and overbite (R= -0.479), although it was not a statistically significant difference. This finding adds to the argument that PP-MP is a valuable measurement to be considered when evaluating vertical jaw relationship and open bite tendencies. Traditionally, PP-MP is under-valued and utilized, and, therefore, the findings of this study should encourage providers to evaluate patients' vertical jaw relationship and open bite tendencies using PP-MP, especially when radiographs without the cranial base are available.

Aim 3

The overall precision of 3D landmark tracing in CBCT was significantly smaller than the overall precision of 2D landmark tracing, 0.550-mm and 1.440-mm, respectively. This finding supports the argument that 3D landmark tracing is more reliable and consistent.

The pattern of inconsistency, however, is different between 2D and 3D. For 2D tracing, a greater portion of the error is observed in the Y-axis, superior to inferior direction than X-axis, anterior to posterior direction. However, this trend is reversed in 3D, where the most significant portion of the tracing inconsistency is observed in X-axis.

Greater inconsistency in Y-axis in 2D may be due to variability that is introduced when the patient either has an asymmetry or had their head in tilted position, which is a known challenge with a 2D lateral ceph. When the subject's head is tilted, it creates superimpositions of bilateral structures in different vertical levels, higher and lower. As the operator tries to determine the middle point of such bilateral structures, variability is likely introduced in vertical axis. On the contrary, 3D tracing's precision in Y-axis is the lowest out of all three axes and is significantly smaller than its counterpart in 2D tracing, at less than 1/5th of its precision value (0.168 vs 0.823 mm).

Evaluation of precision was further dissected by looking into each landmark separately. General ranking of landmarks in the order of overall precision was similar between 3D and 2D as expected. When the unpaired t-test was performed for every landmark evaluated except ANS, the precision value of 3D was significantly lower than 2D. In fact, the ANS ranked last out of all 3D landmarks in precision ranking while ranking third place in the 2D landmarks in precision ranking. The reason why there is no significant difference of ANS precision in 3D and 2D can be directly attributed to precision in X-axis, 0.756-mm and 0.649-mm, respectively. This shows that the sagittal location of ANS is difficult to identify regardless of whether in 3D or 2D. This finding is likely due to the fact that the anatomy of ANS becomes very thin as it approaches the tip of its spine. However, the variability in the sagittal direction does not cause a major concern, as its vertical component is more critical in determining the position of the palatal plane.

Root positions of both upper and lower incisors are one of the landmarks that deviate from the trend of ranking similarly in both 3D and 2D. In 3D, upper incisor root ranks at 3/15 with 0.250-mm precision compared to 6/9 ranking and 1.538-mm precision in 2D. Lower incisor root ranks at 5/15 with 0.464-mm in 3D compared to 7/9 rank and 1.562-mm precision in 2D. Root apices are often challenging structure to identify in lateral cephalographs because there are several structures superimposed on top of each other. Not only are they bilateral structures, but often the root apices of lateral incisors and even canines are superimposed together, making it difficult for the operator to identify them consistently. The improvement in precision of identifying root apices in 3D tracing is because the operator can eliminate the superimposition factor by tracing one apex at a time.

Even further breakdown of each landmark in different axes is useful to understand where the inconsistency is found and to determine if the inconsistency is one that will contribute to measurements or not. As discussed above, ANS's variability in sagittal direction does not alter the position of the palatal plane significantly enough to influence related measurements such as PP-MP or PP-U1 angles.

Crown tips of both incisors ranked near the top in both 3D and 2D. However, closer evaluation of each axis reveals that while most of the inconsistency was found in Y-axis in 2D, the precision value in Y-axis improves greatly in 3D, even becoming smaller than X-axis precision value in upper central incisors. The inconsistency in 3D was mostly due to inconsistency in the Z-axis, likely due to the challenge of finding a midpoint on incisor edge.

Although its overall precision improves to 0.873-mm in 3D from 1.913-mm in 2D, PNS ranked near the bottom in both 3D and 2D . Closer look at each axis reveals that most of the

inconsistency is found in X-axis.   Similarly to ANS, the inconsistency in X-axis is not as critical since it has the least influence on determining the position of the palatal plane.

Gonions and the antegonial notch are two structures that showed greater inconsistency in X-axis more than Y-axis in 2D. This is likely due to the fact that both structures are well-rounded structures without sharp borders or edges, especially along the lower border of the mandible. In 3D, eliminating superimposition via isolating left and right structures improves precision in Y-axis greatly, but not as much improvement is noted in X-axis .

Orbitales were the only landmarks in 3D, which displayed the greater inconsistency in Z-axis than in X- and Y-axes. This can be explained by the anatomy of the orbitale, which extends long in Z-axis. The lack of precision in Z-axis is relatively less critical than other axes because the orbitale-to-orbitale line runs along the Z-axis.

AIM 4

The pattern between 3D and 2D measurements differed between the three measurements: upper incisor to palatal plane (U1-PP), lower incisor to mandibular plane (L1-MP), and palatal plane to mandibular plane (PP-MP). Across 5 subjects, U1-PP angles were consistently smaller in 3D tracing compared to 2D tracing. The average difference was -3.73 degrees, which was statistically significant by Wilcoxon signed rank test.   L1-MP angles were consistently greater in the 3D tracing than 2D tracing. The average difference was 2.35 degrees, which was statistically significant by Wilcoxon signed rank test. Lastly, PP-MP, although was smaller in 3D, was not significantly different by the Wilcoxon signed rank test. Given the findings from Aim 3 of the study, which showed greater precision with 3D landmarks compared to 2D landmarks, especially with incisor root apex position, the current findings of significant difference in these angular

measurement should encourage providers to consider the advantage of 3D tracing and measurements.

CONCLUSION

- PP-MP is similarly as valuable is SN-MP is in studying vertical jaw relationships and open bite tendencies.

- Hybrid of volumetric rendering and multi-planar reconstruction view for 3D tracing of CBCT is an efficient and effective approach.

- Tracing in 3D was significantly more precise in 3D tracing of CBCT than 2D tracing of lateral cephalographs in all landmarks tested except ANS.

- Incisor crown tips ranked at top in precision in both 3D and 2D, while PNS ranked at the bottom in both 3D and 2D.

- Precision of structures with a lot of superimpositions, such as root apices, improved the most significantly, especially in Y-axis (vertical).

- It is important to understand the precision of tracing in an individual axis for different landmarks because some have greater impact on measurements than the other.

- U1-PP measurements from 3D tracing was significantly smaller than that of 2D tracing and L1-MP measurements from 3D tracing was significantly greater than that of 2D tracing.

- In light of present findings, clinicians should utilize palatal plane as a reference plane to evaluate vertical relationship, especially when radiograph with limited field of view is available. Additionally, they should expect to learn and utilize 3D tracing and analyses in the future.

- Future studies can use the 3D tracing protocol developed in the present study to compare and evaluate frontal measurements between CBCT and anterior-posterior cephalographs.

REFERENCES

1. Hounsfield GN. Computerized transverse axial scanning (tomography). Part I. Description of system. Br J Radiol 1995;68:H166-72.

2. Mah JK, Danforth RA, Bumann A, Hatcher D. Radiation absorbed in maxillofacial imaging with a new dental computed tomography device. Oral Surg Oral Med Oral Pathol Oral Radiol Endod 2003;96:508-13.

3. Carlsson CA. Imaging modalities in x-ray computerized tomography and in selected volume tomography. Phys Med Biol 1999;44:R23-56.

4. Mozzo P, Procacci C, Tacconi A, Martini PT, Andreis IA. A new volumetric CT machine for dental imaging based on the cone- beam technique: preliminary results. Eur Radiol 1998;8:1558-64.

5. Ludlow JB, Davies-Ludlow LE, Brooks SL. Dosimetry of two extraoral direct digital imaging devices: NewTom cone beam CT and Orthophos Plus DS panoramic unit. Dentomaxillofac Radiol 2003;32:229-34.

6. Baumrind S, Frantz RC. The reliability of head film measurements 1. Landmark identification. Am J Orthod 1971a;60:111-27.

7. Baumrind S, Frantz RC. The reliability of headfilm measurements. 2. Conventional angular and linear measures. Am J Orthodont 1971b; 60: 505–517.

8. de Oliveira A E, Cevidanes L H, Phillips C, Motta A, Burke B, Tyndall D. Observer reliability of three-dimensional cephalometric landmark identification on cone-beam computerized tomography. Oral Surg Oral Med Oral Pathol Oral Radiol Endod 2009; 107: 256–65.

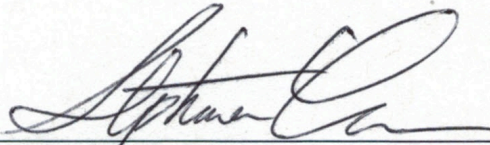9. Lou L, Lagravere MO, Compton S, Major PW, Flores-Mir. Accuracy of measurements and

reliability of landmark identification with computed tomography (CT) techniques in the maxillofacial area: a systematic review. Oral Surg Oral Med Oral Pathol Oral Radiol Endod 2007; 104: 402–11.

10. Houston WJB. The analysis of errors in orthodontic measurements. Am J Orthod 1983;83:382-90.

11. Major PW, Johnson DE, Hesse KL, Glover KE. Landmark identification error in posterior anterior cephalometrics. Angle Orthod 1994;64:447-54.

12. Broadbent B. A new x-ray technique and its application in orthodontia. Angle Orthodontist 1931; 51: 93–114.

13. Trpkova B, Major P, Prasad N, Nebbe B. Cephalometric landmarks identication and reproducibility: a meta analysis. Am J Orthodont Dentofac Orthoped 1997; 112: 165–170.

Publishing Agreement

It is the policy of the University to encourage the distribution of all theses, dissertations, and manuscripts. Copies of all UCSF theses, dissertations, and manuscripts will be routed to the library via the Graduate Division. The library will make all theses, dissertations, and manuscripts accessible to the public and will preserve these to the best of their abilities, in perpetuity.

Please sign the following statement:

I hereby grant permission to the Graduate Division of the University of California, San Francisco to release copies of my thesis, dissertation, or manuscript to the Campus Library to provide access and preservation, in whole or in part, in perpetuity.

_____   6/6/16
Author Signature   Date